THE UNIVERSITY OF MICHIGAN
College of Engineering
Department of Mechanical Engineering
Cavitation and Multiphase Flow Laboratory

Report No. UMICH 03371-19-T

CAVITATION BUBBLE DYNAMICS RESEARCH- THEORY, INSTRUMENTATION, RESULTS

(Presented at Pennsylvania State University Summer Conference on Cavitation , August 1972)

Frederick G. Hammitt*

Financial support for report preparation
by
National Science Foundation
Grant No. GK-1889

June, 1972

*Professor-in-Charge
Cavitation and Multiphase Flow Laboratory

ABSTRACT

The report has been prepared primarily for a Summer Conference at Pennsylvania State University on cavitation. It covers bubble dynamics for compressible, viscous, spherical collapse; and also for non-symmetrical collapse in an incompressible, viscous liquid.

A section on high-speed photography as applied to cavitation research, and one on methods of cavitation damage testing are also included.

TABLE OF CONTENTS

LIST OF FIGURES

FIGURES

I. PHOTOGRAPHIC TECHNIQUES AND CAVITATION

A. Introductory Remarks

Much of the "name of the game" of cavitation research at the present time is its more exact and precise observation, and also detection. This is true because analytical methods are not yet adequate to make unnecessary the direct observation of the phenomenon. Then visual observation, including use of photographic techniques, becomes very important. These techniques are of course limited to container-liquid systems of some degree of transparency. However, we have used in our laboratory photographic studies of cavitating mercury (in a plexiglas venturi) in that the phenomena in the boundary layer adjacent to the plexiglas can be observed. This was the location at which cavitation occurred in this instance.

In general, cavitation is a phenomenon requiring very short exposures, and high framing rates for motion picture cameras, in order to "stop" the flow. Also, what appears to be a relatively "steady-state" cavity to the unaided eye, is often revealed to involve very high rates of motion if studied with high-speed photography, or if simply viewed with the aid of a "strobe" light providing flash durations of only a few microseconds (μs).

While it is difficult to find literature pertinent to this subject, the recent book Cavitation, Knapp, Daily, and Hammitt (1) contains a certain amount of pertinent material. A copy of these pages is appended to the class notes. In the references there listed, that of Hyzer (2) is particularly useful. Some of the major points are further reviewed in this write-up.

B. Requirements for Cavitation Research

1. General Flow Patterns

Historically, the optical resolution of cavitating flows appears to require exposure times no greater than perhaps 10^{-4} seconds and motion picture framing rates of at least 10^{3}. A substantial portion of the early work in regard to cavitation was done by Knapp in the (1940's) at Calif. Inst. of Tech. (1), and utilized equipment newly developed at that time, including drum

type cameras and Kerr-cell light sources. This is described in the pages from ref. 1 appended to the class notes. Framing rates up to 40,000/sec. were acheived. The photography was adequate to view the traverse growth and collapse of individual bubbles, as well as the fluctuating edges of the "vaporous" cavitating region.

C. Trades-Offs and Limitation of High-Speed Photography

1. Parameters of Phenomena

a. Small size (particularly for individual bubbles), order of 1-2 mm, or less.

b. Rapid motions and short duration. Bubble collapse typically occurs in a few milliseconds, but the significant final portion is few microsecond

c. Two phase boundary reflects and refracts light even though both bubble content and liquid may be completely transparent. Hence, this is not an ideal subject for photography, but not an impossible one. Either back-lighting or front-lighting are feasible, and results differ to some extent.

d. Random in time (at least, the bubbles in "natural" cavitation). Hence, it may be necessary to trigger bubbles (or otherwise detect their passage) to trigger the camera and light source.

Since bubbles do not appear in general at fixed time intervals, strobe lighting, as used to study events in rotating machine passages, can not generally be used. Of course, this technique can be used to advantage for study of cavitating flow in pump or inducer passages.

2. Parameters of Camera and Light Source

a. General- For still shots of exposures less than $\sim 10^{3}$ sec., mechanical shuttering is, of course, not practical to control exposure time. Rather, light source duration is used. Th flash occurs during the period while the mechanical camera shutter is open. This is also conventional practice for standard cameras and flash bulbs where a 1/30 sec. mechanical shutter setting is used.

The remaining discussion applies particularly to high-speed motion picture cameras.

b. High Speed Motion Picture Camera Parameters

The limiting parameters of the high speed motion picture camera are:

1) Framing rate (max. and min.)

2) Exposure time per frame which is not necessarily directly related to reciprocal of framing rate.

3) Lens capability (light impinged on film for given light source arrangement).

4) Number of frames possible per run.

5) Magnification of field viewed, depth of field; function of built-in lens system and external lenses.

6) Film type, resolution vs. light requirement, "graininess" of film.

c. Light Source Parameters

1) Total energy per pulse.

2) Duration of pulse.

3) Possible repetition rate.

d. Interplay between Parameters

1) Framing rate and Number of Frames- Since in many cases the number of frames is inconveniently small, use of maximum framing rate gives minimum time sampled. The latter may be then inconveniently small.

2) Framing Rate and Exposure Time-Not related if a pulsed light source is used to give the exposure times. If only the shuttering mechanism of camera is used, then clearly a low framing rate may result in too long an exposure time to get sharp pictures.

3) Lens capability, magnification, depth of field, size of field are obviously all related in known but complex ways.

D. Present High Speed Motion Picture Camera Types

1. Fastax Type

a. Mechanical shutter as "conventional" camera, film is pulled past shutter. Film rolls are of standard length.

b. 10,000-15,000 frames/sec.

c. Exposure time $\leq$ 1/framing rate, unless a synchronized pulsed light source is used. Such is available up to $\sim$ 8000/sec., from Edgerton, Germeshausen, and Grier.

d. "Unlimited" film length. Thus, with this type of camera there is a reduced problem with random events, but an increased cost for film processing.

e. Relatively poor optics.

f. $5000-$10,000 including light source.

2. Dynafax (Beckman-Whitley) Type

a. No mechanical shutter, film in drum which rotates around camera axis. Rotating prism on axis directs light toward film drum. Local lens systems focus on the moving film and give the shuttering effect.

b. 25,000-40,000 frames/sec.

c. Exposure time $\leq$ 1/framing rate.

d. Limited film length (about 100 frames), and hence limited sampling time.

e. Improved optics compared to Fastax.

f. $10,000-$15,000 including light source.

3. Ultra High-Speed Drum Camera

(Beckman-Whitley, Cordin, Barr-Stroud)

a. Similar to Dynafax except film is stationary in circumferential drum.

b. ($.1 \times 10^6$ to 10×10^6 frames/sec.

c. Exposure time $\leq$ 1/framing rate.

d. Limited film length (about 80 frames)

e. Optical quality similar to that of Dynafax

f. $50,000 with light source

4. Cranz - Schardin Type

a. Multiple sparks, arranged in circle, provide corresponding exposures on large stationary film plate. Only silhouette lighting possible. Number of pictures is equal to number of sparks; hence limited to $\sim$12 frames.

b. Framing rate up to $\sim 10^6$/second

c. Exposure time not coupled to framing rate, depending only on design of individual spark circuits.

d. Not available commercially in USA, but may be available in Europe. Can be constructed for ~$1000. We have built and used this type of camera in our laboratory.

5. Image Conversion (Electronic) Camera- Process somewhat like TV. Framing rate can be in the nanosecond range (2×10^7 for "Imacon"), but number of frames is limited. Commercial model ("Imacon"), distributed by John Hadland in U. K., claims 4-20 images. I believe optical qualities such as resolution are poor compared to conventional cameras. I have no information on price.

Our laboratory has used high speed motion picture photography considerably for the study of both cavitation and boiling bubble behavior. A short movie of bubble growth and collapse in a venturi taken at $\sim 0.5 \times 10^6$ frames/second with our Beckman-Whitley drum camera, is presented here as representative. A full description of the background material for this movie is given elsewhere (13). Back lighting was used. Bubbles are collapsing near a wall and in a positive pressure gradient, and their collapse is affected by both of these factors. Some descriptive literature on high-speed cameras is available (and will be circulated at conference).

II. BUBBLE DYNAMICS FOR COMPRESSIBLE FLUID

A. Introductory Remarks

Previous lectures in this conference have considered bubble collapse under conditions of spherical symmetry in an incompressible fluid. However, detailed numerical calculations[1, 4, 6, e.g.] show that the bubble wall velocities can easily approach substantial Mach numbers with regard to the speed of sound of the undisturbed liquid, and could well become highly supersonic in this regard if spherical symmetry were maintained. Under these conditions, then, the compressibility of the liquid must importantly influence the wall velocity near the conclusion of collapse, if spherical symmetry is maintained. While actual photographic evidence as well as theory show that such symmetry is seldom maintained under conditions encountered in practice, so that high liquid Mach numbers will be achieved, it is desirable to investigate the effects of compressibility (a moderation of pressure and velocity) and of various sources of non-symmetry. Both of these will be considered in this Chapter. In addition, some consideration will be given to the impact between the "microjet" generated in asymmetric bubble collapse and the wall material.

B. Compressible Viscous Fluid with Spherical Symmetry

1. General Formulation

We will start with a consideration of the general equations, following the thesis by Ivany[4] at the University of Michigan. The equations are numbered according to that source.

$$\frac{D\rho}{Dt} = \rho \operatorname{div} \vec{V} = 0 \quad \left(\text{or } \operatorname{div} \rho \vec{V} = -\frac{\partial \rho}{\partial t}\right) \qquad \ldots(1)$$

$$\frac{D\vec{V}}{Dt} = -\frac{\operatorname{grad} p}{\rho} + \frac{\mu}{\rho}\left[\nabla^2 \vec{V} + \frac{1}{3} \operatorname{grad}(\operatorname{div} \vec{V})\right] \qquad \ldots(5)$$

Consider a compressible viscous fluid with spherical symmetry. Now by spherical symmetry, curl $\vec{V} = 0$, and there is a vector identity,

$$\nabla^2 \vec{V} = \text{grad}\,(\text{div}\,\vec{V}) - \text{curl}\,(\text{curl}\,\vec{V})$$

Use this to eliminate 1st term in bracket in (5):

$$\frac{D\vec{V}}{Dt} = -\frac{\text{grad}\,p}{\rho} + \frac{4}{3}\,\frac{\mu}{o}\,\left[\text{grad}\,(\text{div}\,\vec{V})\right]$$

now substitute (1) to get:

$$\frac{D\vec{V}}{Dt} = -\frac{\text{grad}\,p}{\rho} + \frac{4}{3}\,\frac{\mu}{\rho}\,\overbrace{\left[\text{grad}\,(-\frac{1}{\rho}\,\frac{D\rho}{Dt})\right]}^{=0} \qquad \ldots(26)$$

Now Gilmore[3] and also Ivany[4] assume that a term involving the cross product between viscosity and compressibility is negligibly small, since both alone are reasonably small.

We come back now to the Euler equation:

$$\frac{D\vec{V}}{Dt} = \frac{\text{grad}\,p}{\rho}$$

and compressibility remains to be considered in the continuity relation, Eq. (1). Now Gilmore assumes the liquid to be barotropic so that $p = p(\rho)$ only, and then $\text{grad}\,p/\rho = \text{grad}\,(p/\rho)$.

Now define an enthalpy term:

$$h(p) = \int_{p_\infty}^{p} \frac{dp}{\rho} \quad ,$$

i.e., we are assuming that the internal energy portion of the enthalpy does not vary, and can be left out of the equations.

Then $(\text{grad}\,p)\,\rho = \text{grad}\,(p/\rho) = \text{grad} \int_{p_\infty}^{p} dp/\rho = \text{grad}\,h(p)$.

Eq. (26) now, in spherical coordinates, becomes:

$$\frac{D\vec{V}}{Dt} = -\frac{\partial h}{\partial r} \qquad \ldots(28)$$

Define pressure wave velocity: $C^2 = \frac{dp}{d\rho}$

From definition of h: $\frac{dh}{dp} = \frac{1}{\rho}$

From the continuity equation, Eq. (1):

$$\frac{D\rho}{Dt} = \frac{d\rho}{dh}\frac{Dh}{Dt} = \frac{Dh}{Dt}\left(\frac{d\rho}{dp}\right)\left(\frac{dp}{dh}\right) = \frac{Dh}{Dt}\left(\frac{\rho}{C^2}\right) \tag{30}$$

So that the continuity equation becomes:

$$-\frac{1}{C^2}\frac{Dh}{Dt} = \text{div}\ \vec{V} \tag{31}$$

Eq. (28) and (31) give 2 partial differential equations with 3 dependent variables V, h, c, and 2 independent variables (r, t). Use of an equation of state for the liquid reduces the dependent variables to 2, so that the partial differential equation set vsn be solved. This has been accomplished by various authors using various assumptions (Flynn, Mellen, Schneider, Brand, e.g., see ref. 4). The most complete numerical work is that by Hickling and Plesset (6), for the compressible case, who made a direct attack on the governing equations without further assumptions. However, they did not include viscosity or surface tension. Ivany (4) also included viscosity and surface tension, which come in through the boundary conditions in Eq. (28), though the cross-product of viscosity and compressibility was neglected in Eq. (26).

2. Equation of State: Following Gilmore, (3), we assume Tait's Eq. of State (25), 1888, for a liquid. A recent literature search we have made (13) indicates this to be still the most sutiable relation for this purpose; using recently determined values of B and n.

$$\left(\frac{p+B}{P_o+B}\right) = \left(\frac{\rho}{P_o}\right)^n \tag{37}$$

where p_o and ρ_o are reference pressure and density. For cold water:
$B \cong 3.05$ kilobars, and $n \cong 7.15$.
We can now compute C^2 in terms of p and ρ, and also h.

$$C^2 = \frac{dp}{d\rho} = \frac{n(p+B)}{p_r}\left(\frac{p+B}{p_r+B}\right)^{-1/n} = \frac{n(p+B)}{\rho} \tag{38}$$

Since p_r and ρ_r are negligible compared with B, and we can show that:

$$h = \frac{n(p_\infty + B)}{(n-1)\,\rho_\infty}\left[\left(\frac{p+B}{p_\infty + B}\right)^{\frac{n-1}{n}} - 1\right] \qquad (39)$$

Now we have eliminated h and C from the equations, but have added p and ρ. However, they are related also by Eq. (37), so that now the dependent variables are p, ρ, and V, and there are three equations.

3. Kirkwood - Bethe Approximation: These can be tackled numerically, and this was the procedure of Plesset (6). However, Ivany (4), following Gilmore (3), used the Kirkwood-Bethe assumption which originates from World War II observations on underwater explosions. They assumed that the quantity, or "characteristic," $r(h + u^2/2)$ is propagated outward with characteristic velocity (C+u) where C = local pressure wave (here sonic) velocity, i.e., the quantity $r(h + u^2/2)$ radiates outward at constant amplitude, so that actually $(h + u^2/2) \propto 1/r$ in the fluid. In the acoustic approximation, where C = const, $p \propto 1/r$ in the fluid, and is propagated outward at velocity, C. Thus some account is taken of compressibility, and the fact that $u \tilde{=} 0$ as compared to C. Thus the speed of propagation is C + u, instead of merely C (as had been assumed in earlier simpler work such as that by Herring and also Trilling, see ref. (1) for discussion of these and other earlier work.), and C varies with p + o. This local C was used in Ivany's calculation (4). We can write the wave equation for the quantity propagated, i.e.:

$$\frac{\partial}{\partial t}\left[r\left(h + \frac{u^2}{2}\right)\right] + (C + u)\frac{\partial}{\partial r}\left[r\left(h + \frac{u^2}{2}\right)\right] = 0 \qquad (32)$$

Using spherical coordinates, $D(\ )/Dt = \frac{\partial(\ )}{\partial t} + u\frac{\partial(\ )}{\partial r}$. Then eq. (32) becomes:

$$\frac{D}{Dt}\left[r\left(h + \frac{u^2}{2}\right)\right] = -C\frac{\partial}{\partial r}\left[r\left(h + \frac{u^2}{2}\right)\right] \qquad (34)$$

from which:

$$r\frac{Dh}{Dt} + ru\frac{Du}{Dt} + (C+u)\left(h + \frac{u^2}{2}\right) + rC\frac{\partial t}{\partial r} + rCu\frac{\partial u}{\partial r} = 0 \qquad (35)$$

Eq. (35) is the Kirkwood-Bethe propagation equation in the proper form for the present purpose. Now we want to substitute Eq. (28) and (31) into (35):

We write the equation for the bubble wall using capital letters to denote this position:

$$RU\frac{dU}{dR}\left(1 - \frac{U}{C}\right) + \frac{3}{2}U^2\left(1 - \frac{U}{3C}\right) = H\left(1 + \frac{U}{C}\right) + \frac{RU}{C}\frac{dH}{dR}\left(1 - \frac{U}{C}\right) \qquad (36)$$

4. Boundary Conditions: We also have a boundary condition at the bubble wall.

$$P(R) = P_i(R) - \frac{2\sigma}{R} - \frac{4\mu U}{R} - \frac{4\mu U}{3C^2}\frac{dH}{dR} \qquad (40)$$

This is then the compressible version of the viscous Rayleigh relation, which is:

$$P(R) = P_i(R) - \frac{2\sigma}{R} + 2\mu\frac{\partial u}{\partial r}$$

$P_i(R)$ can be assumed to be any function of R such as, e. g., the perfect gas assumption. The last term in Eq. (40) was neglected by both Gilmore and Ivany Gilmore found it to be of the same order as the product of viscosity and compressibility, which was also neglected. Substituting the equation of state results (Eq. 38, 39) into Eq. 36 to eliminate h + C. This gives a final equation to be solved, which has only one dependent variable, U and the independent variable, R. The boundary condition is P(R) at the bubble wall. All this can be only done numerically of course.

5. Calculations of Pressures and Velocities in Liquid: In the case of Ivany (4), and Gilmore (3), the pressures and velocities in the liquid are calculated, using the Kirkwood-Bethe hypothesis, and theory of characteristics. There is a quantity $z = z(r,t) = r(h + u^2/2)$ which is constant along a path or characteristic, traced by a point moving with velocity (C + u), as shown in the sketch (next page).

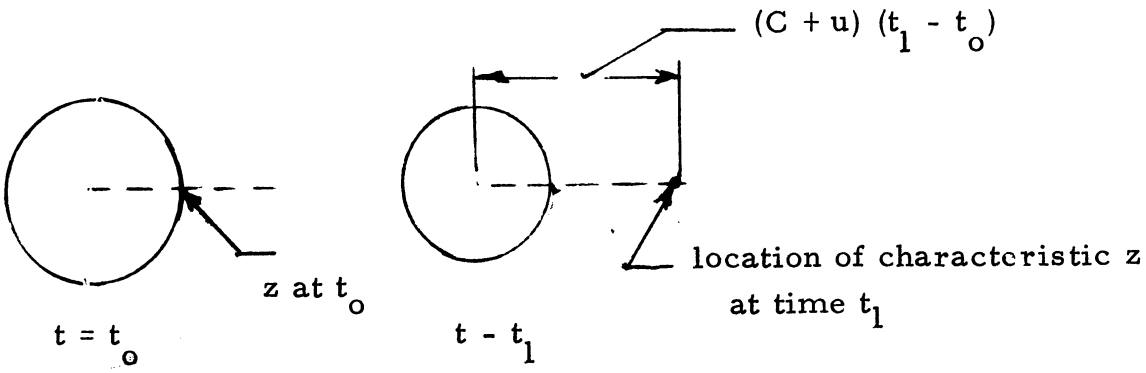

Along a path in the r-t plane the rate of change of any variable:

$$\left(\frac{d(\ )}{dt}\right)_c = \frac{\partial(\ )}{\partial t} + \frac{\partial(\ )}{\partial r}\frac{dr}{dt} = \frac{\partial(\ )}{\partial t} + \underbrace{(C + u)}_{= \frac{dr}{dt}}\frac{\partial(\ )}{\partial r}$$

where subscript c signifies the derivative along a characteristic. It then can be shown that:

$$p(r,t)_c = (p_\infty + B)\left[\left(\frac{z}{r} - \frac{u^2}{2}\right)\left(\frac{n-1}{n}\right)\left(\frac{\rho_\infty}{p_\infty + B}\right) + 1\right]^{\frac{n}{n-1}} = B \qquad (48)$$

where $z = r\left(h + \frac{u^2}{2}\right)$

Figures showing some of the significant results follow.

C. Asymmetric Bubble Collapse

1. Present Knowledge and State of Art (11)

a) A growing bubble is stable because of the $1/r^2$ effect, even thoug the lighter fluid is accelerating into (or toward) the heavier, preventing instability this case, even though it would be expected under the G.I. Taylor analysis for plane surfaces. However, by the same token, the collapsing bubble is unstable.

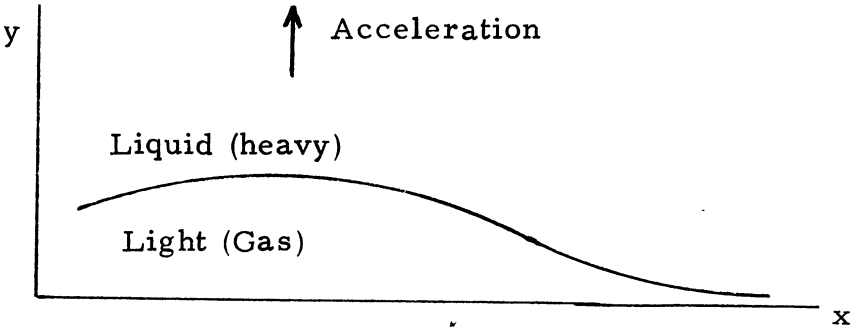

Unstable if gas accelerates into liqui

Under this situation, the "bumps" will grow because a given Δ y gives the same Δ p in either fluid, and thus a greater acceleration in the lighter fluid. Hence, gas in the concave side of the bump will push faster into the liquid.

b) The collapsing bubble is unstable, primarily because of the geometric effect, ($1/r^2$ effect). However, this is a rather weak instability, and only applies after a fairly considerable R/Ro has been attained.

c) In any case, actual situations always involve a real asymmetry s as gravity, pressure gradient, velocity, or velocity relative gradient relative to t bubble presence of a nearby wall, etc.

2. Wall Proximity Case: The case of a bubble collapsing in close proximity to a wall will be considered as an example.

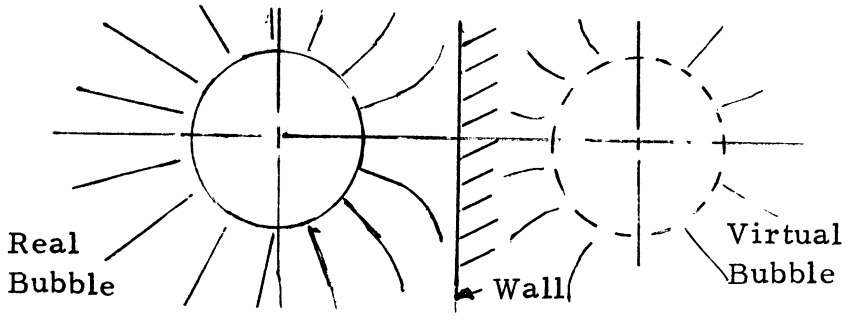

The boundary condition at wall is that v = 0 and u= 0. If we replace the wall by a virtual bubble (or source or sink) behind the wall these conditions are met. Then

each bubble (virtual and real) moves in the induced velocity formed by the other, so that the real bubble moves toward the wall. Then R = U on the wall side is smaller, so that the bubble appears to move toward the wall as it collapses (vice versa for a free surface). Since R is R (O), the collapse is not symmetrical. Actually, the bubble is drawn toward the wall and flattens in a direction parallel to the wall, generating a torus and jet directed toward the wall. A "soft" wall or free surface reverses this behavior, because a sufficiently soft wall would be "sucked" out toward the bubble.

3. Collapse of Hemispherical Bubbles on Wall

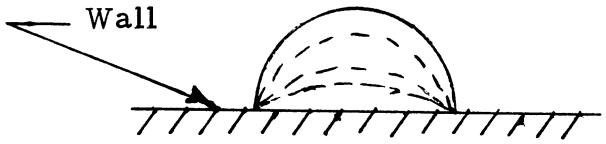

The end points on the wall are static so R = R (Θ) and R(C) C = 0 and 180°. (This arguement relies on fluid friction). The complete analysis is found in ref. 8.

4. Asymmetric Bubble Dynamics (Numerical Approaches): Possible approaches to this problem exist, as listed and discussed below.

a) Ideal Flow (Potential Function and Expansion of the surface in Legendre Polynomials) is used.

$$\phi = \frac{R^2 \dot{R}}{r} + \sum_{n=1}^{\infty} \frac{b_n P_n \cos\theta}{r^{n+1}}$$

$$R = (\theta,t) = R_o(t) + \sum_{n=1}^{\infty} a_n(t) P_n \cos\theta$$

1.) This expansion was used by Plesset, etal. (7), to determine whether perturbations would grow or damp. In growth, the $1/r^2$ geometric effect overwhelms the unstable terms as $r \to \infty$.

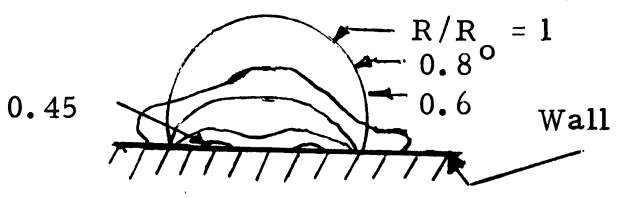

This is really an exact solution if the number of terms in the Legendre polynomial is infinite, but it is a "small perturbation" analysis, (i.e., linearized)

2.) Yeh-Yang Analysis (10)

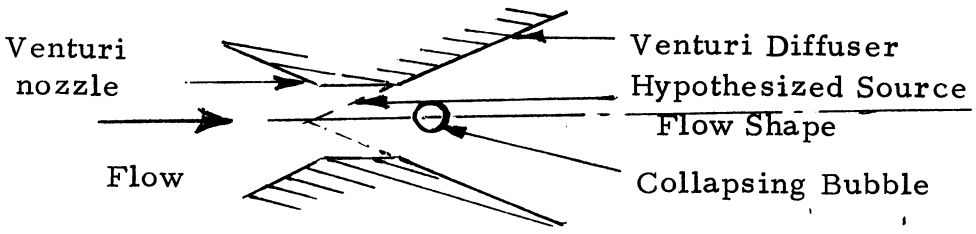

They showed for a critical initial bubble velocity for $V_b > V_{crit}$, the bubble progresses faster into the diffuser as it collapses, and vice-versa. The direction of the jet formed in the bubble collapse depends on the relative bubble velocity as has also been observed photographically (13).

3.) Modified Program for Asymmetric Bubble (11)

General Equations

$$\nabla \cdot \vec{u} = 0$$

$$\frac{\partial \vec{u}}{\partial t} = -(\vec{u}\cdot\vec{\nabla})\vec{u} - \nabla P$$

$$(\vec{u}\cdot\nabla)\vec{u} = \vec{\nabla}\cdot(\vec{u}\cdot\vec{u}) - \vec{u}(\nabla\cdot\vec{u})$$

$$D = \vec{\nabla}\cdot\vec{u}$$

$$\frac{\partial D}{\partial t} = -\nabla^2 P - [\vec{\nabla}\cdot\vec{\nabla}\cdot(\vec{u}\cdot\vec{u})]$$

For spherical symmetry:

$$\frac{\partial u}{\partial t} + \frac{1}{2}\frac{\partial}{\partial r}(u^2) = -\frac{\partial P}{\partial r}$$

$$\frac{1}{\delta t}\left(u^{n+1}_{i+\frac{1}{2}} - u^{n}_{i+\frac{1}{2}}\right) = \frac{1}{2}\left(\frac{u_i^2 - u_{i+1}^2}{\delta r}\right) + \left(\frac{P_i - P_{i+1}}{\delta r}\right)$$

$$t = n\cdot\delta t \qquad t + \delta t = (n+1)\delta t$$

$$\frac{1}{\delta t}\left(D_i^{n+1} - D_i\right) = \frac{1}{(\delta r)^2}\left[r_{i+\frac{1}{2}}\left(P_i - P_{i+1}\right) - r^2_{i-\frac{1}{2}}\left(P_{i-1} - P_i\right)\right] +$$

$$+ \frac{1}{\delta r^2}\left[\frac{r_{i+\frac{1}{2}}}{2}\left(u_i^2 = u_{i+1}^2\right) - \frac{r^2_{i-\frac{1}{2}}}{2}\left(u^2_{i-1} - u_i^2\right)\right]$$

Note that D = O but D $\neq$ 0 due to numerical approximations. Hence, the objective is to get D to approach zero as closely as possible.

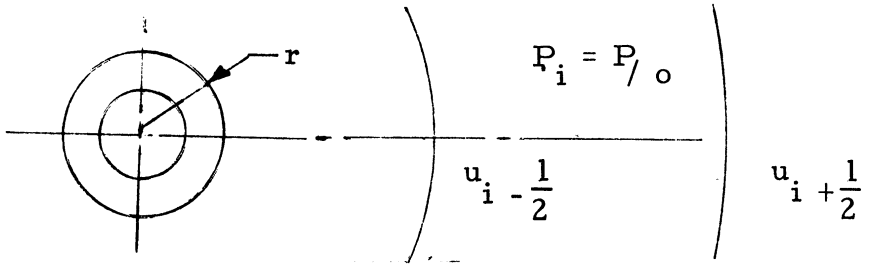

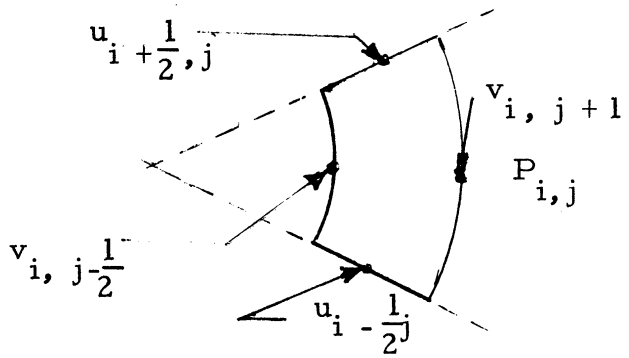

Fig. (1-3) showing some of the significant results follow.

D. Droplet or Jet Impact

1. Introductory Remarks: Certain major points are evident and can be listed as below.

a. An asymmetric cavitation bubble collapse often generates a "micr jet" which may impinge upon a nearby wall, particularly in those cases where an adjacent wall is the asymmetry in question, thus contributing to damage. This will aid and abet shock-wave imposition on the same portion of the wall, particularly during bubble rebound, as previously discussed, and shown by ours (13) and other motion pictures of cavitation bubble behavior.

b. Cavitation erosion and impingement erosion have very similar appearance, strengthening the hypothesis of the importance of the microjet impact phenomenon in cavitation erosion.

c. Liquid droplet impact is an important field in its own right in such applications as wet steam droplet impingement on blades in large steam turbines and rain erosion of high-speed aircraft and missile components.

2. Simplified Impact Analysis

a. "Slab" Collision -- The simplest case to be considered is that of the collision between an infinite liquid "slab" and an infinite rigid solid. In this case, the "water hammer" relation applies, i.e., the water hammer pressure,

$$\Delta P = \rho C V, \qquad (1)$$

where C = sonic velocity in liquid

V = impact velocity

and ρ = liquid density

i. "Compressibility" of liquid must be considered to get non-trivial results. If liquid were incompressible, C = infinity and ΔP becomes infinite. Hence no useful results can be achieved without considering a finite compressibility of the liquid.

ii. If the inevitable compressibility of the solid is also considered, then ΔP is somewhat reduced in that the acoustic impedance ratio between liquid and solid becomes involved, so that

$$\Delta P = \frac{\rho C V}{\frac{1 + (AI)_{solid}}{1 + (AI)_{liquid}}} \qquad (2)$$

where $(AI)_{solid} = \rho_s C_s$ = "Acoustic Impedance"

iii. If the increased shock wave velocity in the liquid (and solid) are considered during impact, ΔP is increased substantially. Actually, we need an equation of state for the liquid, of which Tait's Equation (24), (previously discussed), is a good example:

$$\left(\frac{p + B}{p_o + B}\right) = \left(\frac{\rho}{\rho_o}\right)^n \qquad (3)$$

Using (3) with the definition of the sonic velocity, $C = (\partial p/\partial \rho)^{1/2}$ we can derive a semi-empirical expression adequate for the purpose. This can then be checked against test results giving the following:

$$\frac{C}{C_o} = (1 + 2V_o/C_o) \qquad (4)$$

from Heymann (14) which is good to liquid Mach Number $V_o/C_o \lesssim 1.2$

A more accurate expression to higher Mach Number $(\lesssim 3)$ from Huang (14) is:

$$\frac{C}{C_o} = 1 + 2\frac{V_o}{C_o} - 0.1\left(\frac{V_o}{C_o}\right)^2 \qquad (5)$$

Using the simpler Heymann expression, Eq. (4) for illustrative purposes, note that for liquid Mach Number, $V_o/C_o = 0.5$, i.e., $V_o \cong 2000$ f/s the shock wave velocity is twice the sonic velocity in the undisturbed liquid. Thus the impact pressure is more than twice that calculated from the classical water hammer equation (Eq. 1), since the liquid density in the impact region is also slightly increased.

b. Geometrical Effects

i. Infinite Slab (of infinite depth). Let us consider in detail the fluid behavior during collisions, starting with a "slab" impact, which is the simplest case to consider. At the instant of impact, the pressure in the liquid layer on the surface rises to the approximate "water hammer" pressure. This high-pressure region is bounded by a "shock-wave" which penetrates into the fluid at shock-wave velocity (somewhat greater than sonic velocity). If the slab is of infinite depth as well as area, this condition will continue indefinitely, since the shock wave will encounter no boundary from which to reflect.

ii. Infinite Slab (of finite depth).

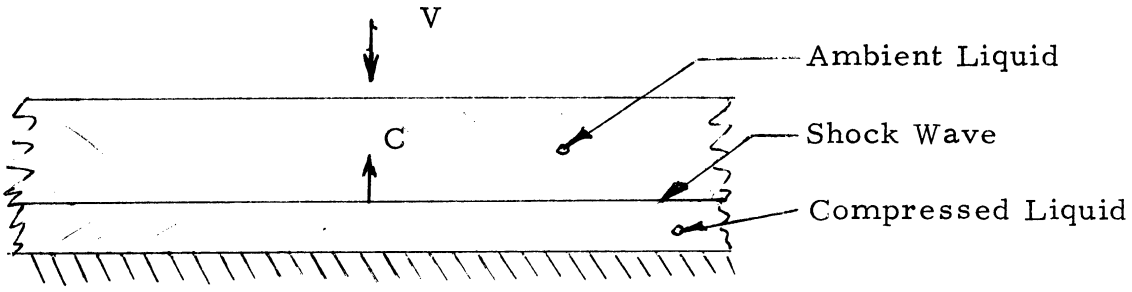

In this case the shock wave will traverse the entire impacting liquid slug, at which point all the liquid will be in the compressed condition. The pressure will then be reflected from the free surface as a rarefaction wave which will decompress the fluid to the ambient condition until it reaches the solid surface. It will then be reflected as a compression wave again from the solid surface, and the process would ideally be repeated indefinitely. This would require the surface to be entirely rigid, C = ∞, Acoustic Impedance = ∞.

III. CAVITATION TEST DEVICES

A. Introductory Remarks

1. Realism of Tests

a. Mechanical and Chemical Effects; Field vs. Test Device: It is very difficult to realistically model this combination of causes and effects. If the test is not at all "accelerated", nearly complete realism may be realized, but there is little economic justification for such a test, since test times would be extremely long. Most "accelerated" cavitation tests involve an accelerated mechanical effect, which then cannot easily be matched by an appropriately accelerated chemical effect.

b. Flowing vs. Non-Flowing Devices: Important effects, primarily velocity, cannot be investigated in non-flowing devices. The effect of pressure, intimately coupled with the velocity effect, then also perhaps cannot be realistically investigated in non-flowing devices.

c. Impact vs. Cavitation Devices: Since cavitation damage is closely related to droplet or jet impact devices, direct impact tests have been used since the 1930's to rate materials for cavitation resistance, and vice-versa.

B. Damage Test Devices: The listing of devices below starts with those probably least "accelerated" and hence probably most realistic. Much description of these is included in the recent book Cavitation (1). Pertinent pages are attached to the summer conference notes.

1. Flowing Devices

a. Simple Venturi (U-Mich. tests, Bangalore Institute of Tech.)

b. Modified Venturis: Provide more rapid erosion, but more complicated flow pattern (Hobbs at NEL; Shalnev, USSR, etc.)

2. Rotating Disc Device: This too is a "flowing system" in a sense, but the flow pattern is very complex. Device consists of flat disc rotating in liquid. Holes in disc (or bosses) provoke cavitation upon specimens embedded in the disc (Naval Applied Sci. Lab., Lichtman (22, e.g.); Pratt and Whitney Aircra Wood (23), e.g.).

3. Vibratory (Non-Flow) Devices: This is the simplest and most economical test, but probably least realistic. Effects of pressure and temperature can be investigated with a variety of fluids in some test facilities, such as e.g. that in our oun laboratory at U-Mich.

The operating principle is that the vibration of a specimen under a test liquid (as water) provides very large accelerations, but only very small velocity, since the amplitude of vibrations is very small ($\sim 2 \times 10^{-3}$ in.). Large accelerations assure rupturing of the liquid, and hence bubbles are created. These are then collapsed by the very high pressure resulting from the return stroke.

C. General Characteristics of Cavitation Damage

1. Macroscopic Appearance (see Fig. 8, 9, descriptions and pictures also in Ref. 1.)

2. Single-Blow Effects (Fig. 10, descriptions and pictures also in Ref. 1.)

3. Macroscopic Effects: These are usually created by an overlay of many individual blows, some creating permanant craters and some only sufficient to cause fatiguing of the surface. Eventually this situation may lead to large

scale fatigue failures of the surface giving very rough surface and macroscopic material removal. Corrosion effects are more or less involved depending on material and fluid. The combined effects of mechanical and chemical attack are much greater than the simple addition of the two acting separately. General appearance is very similar to droplet impingement damage. Macroscopic effects can be produced such as the actual bending of propellor or turbine blades (1, 16,17).

D. Cavitation Damage Research

1. Single-Blow vs. Multiple Event Approach: Both avenues have been and are continually being followed.

2. Single-Event Studies

a. Photography and Visualization: Movies such as that of bubbles in venturi collapsing adjacent to an aluminum plate are of great utility in this regard, shown previously in this conference. Also, numerical studies are possible such as those for which the results are shown in a short movie taken from computer results from the Ph.D. thesis by Mitchell (11) in our laboratory, using a modified MAC program. Curves of typical results are attached to the conference notes. This work, discussed previously, included the study of the effects of wall proximity, pressure gradient, and external flow velocity. Viscous effects within the fluid were included. Similar results for the wall proximity case in an inviscid fluid were obtained by Chapman (Ph.D. thesis) at Calif. Inst. Tech. (18,19), using a different program. However, their results were carried further for this particular case, showing the actual development of the "microjet."

3. Multiple Event Studies: The single event studies cannot yet predict macroscopic erosion effects such as that of velocity, pressure, temperature, etc. Thus direct damage tests are necessary in these regards. Some such results, particularly from a vibratory facility at the Univ. of Mich., on the effects of pressure, temperature, and fluid will be illustrated by slides. Typical results are shown in curves attached to the conference notes (Fig. 14-17). They have been reported previously (20,21). In addition, some work illustrating effect of velocity for a rotating disc facility at Pratt and Whitney, in which the author participated (23) shows the effect of velocity and will be discussed (Fig. 23) in the oral presentation.

This concludes the formal presentation, but I would now like to show our short movie of computer results, previously mentioned. Considerable additional related results I believe will be presented by the next speaker.

IV. APPENDIX

A. Photographic Techniques

The following material is appended to the Conference Notes, pertinent to this subject.

1. Title page and pp. 35-41 and 47-50 of R. T. Knapp, J. W. Daily, and F. G. Hammitt, Cavitation, McGraw-Hill, 1970 (Ref. 1 of this report).

B. Bubble Dynamics

1. "Thermodynamic" Effects in Cavitation Damage. The "thermodynamic effect" in our tests (24) is best described by a B_{eff} parameter adapted from Florschuetz and Chao (25)

$$B_{eff} = \left(\frac{\rho_L C_L \Delta T}{\rho_v h_{fg}}\right)^2 \left(\frac{\kappa_L}{R_o}\right) \left(\frac{1}{NPSH}\right)^{1/2}$$

where NPSH = 1 ft and R_o = 1 cm to obtain relative values for comparison between different fluids and materials.

2. The following material is appended to the Conference Notes, pertinent to this subject.

   a. Pp. 112-132 and 149-152 of Ref. 1.

   b. ASME paper, Ref. 4, Ivany and Hammitt.

   c. Physics of Fluids article, Ref. 6, Hickling and Plesset.

C. Cavitation Test Devices and Results

The following materials, pertinent to this subject, is appended to the Conference Notes.

1. Pp. 375-443 of Ref. 1.

REFERENCES

1. R. T. Knapp, J. W. Daily, and F. G. Hammitt, Cavitation, McGraw-Hill, New York, 1970.

2. W. G. Hyzer, "Engineering and Scientific High Speed Photography," MacMillan Company, 1962.

3. F. R. Gilmore, "Growth or Collapse of a Spherical Bubble in a Viscous Compressible Liquid," Report No. 26-4, April 1, 1952.

4. R. D. Ivany and F. G. Hammitt, "Cavitation Bubble Collapse in Viscous Compressible Liquids-Numerical Analysis," Trans. ASME, 87, D, J. Basic Engr., 977-985, 1965; see also R. D. Ivany, Ph.D. Thesis, Nucl. Eng. Dept., The University of Michigan, 1965.

5. F. G. Hammitt and W. Smith, "Bubble Dynamics," Nuclear Engr. Dept., The University of Michigan, 1964.

6. R. Hickling and M. S. Plesset, "Collapse and Rebound of a Spherical Bubble in Water," Physics of Fluids, 7, 7-14, 1964.

7. M. S. Plesset, "On the Stability of Fluid Flows with Spherical Symmetry," J. Appl. Phys., 25, 96-98, 1954; see also M. S. Plesset and T. P. Mitchell, "On Stability of Spherical Shape of Vapor Cavity in Liquid," Quart. Appl. Math, 13, 419-430, 1956.

8. C. F. Naudé and A. T. Ellis, "On the Mechanism of Cavitation Damage by Nonhemispherical Cavities Collapsing in Contact with a Solid Boundary," Trans. ASME, 83, D, J. Basic Engr., 648-656, 1961.

9. N. D. Shutler and R. B. Mesler, "A Photographic Study of the Dyanmics and Damage Capabilities of Bubbles Collapsing Near Solid Boundaries," Trans. ASME, 87, D, J. Basic Engr., 511-517, 1965.

REFERENCES (Continued)

10. H.-C. Yeh and W.-J. Yang, "Dyanmics of Bubbles Moving in Liquids with Pressure Gradient," J. Appl. Phys., 39, 3156-3165, 1968.

11. T. M. Mitchell, "Numerical Studies of Asymmetric and Thermodynamic Effects on Cavitation Bubble Collapse," Ph.D. Thesis, Nucl. Engr. Dept., The University of Michigan, 1970; see also T. M. Mitchell and F. G. Hammitt, "Asymmetric Cavitation Bubble Collapse," to be presented ASME Winter Annual Meeting, 1972.

12. J. E. Welch and F. H. Harlow, et al., "A Computing Technique for Solving Viscous, Incompressible, Transient Fluid-Flow Problems Involving Free Surfaces," Los Alamos Sci. Lab., LA-3425, 1966.

13. C. L. Kling, "A High Speed Photographic Study of Cavitation Bubble Collapse," Ph.D. Thesis, Nuclear Engr. Dept., The University of Michigan, 1970; see also C. L. Kling and F. G. Hammitt, "A Photographic Study of Spark-Induced Cavitation Bubble Collapse," Trans ASME, J. Basic Engr., 1972, ASME Paper No. 72-FE-20.

14. Y. C. Huang, "Numerical Studies of Unsteady Two-Dimensional Liquid Impact Phenomena," Ph.D. Thesis, Mech. Engr. Dept., The University of Michigan, 1971.

15. Y. C. Huang, F. G. Hammitt, and W.-J. Yang, "Hydrodynamic Phenomena During High Speed Collision Between Liquid Droplet and Rigid Plane," (submitted ASME), ORA Rept. UMICH No. 03371-12-T, May 1972, The University of Michigan, Ann Arbor, Michigan.

REFERENCES (Continued)

16. J. D. VanManen, "Bent Trailing Edges of Propellor Blades of High-Powered Single-Screw Ships," Int. Ship Building Progress, 10, 101, 3-7, January 1963.

17. E. Makay, "Flow Instabilities in High-Speed Centrifugal Pumps," Franklin Institute Research Laboratory, 32-TR-70-1, 1971.

18. R. B. Chapman, "Nonspherical Vapor Bubble Collapse," Ph.D. Thesis, Cal. Inst. Tech., 1970.

19. M. S. Plesset and R. B. Chapman, "Collapse of an Initially Spherical Vapor Cavity in the Neighborhood of a Solid Boundary," J. Fluid Mech., 2, 47, p. 283, May 1971.

20. F. G. Hammitt and D. O. Rogers, "Effects of Pressure and Temperature Variation in Vibratory Cavitation Damage Test," J. Mech. Engr. Sci., 12, 6, 432-439, 1970.

21. F. G. Hammitt and N. R. Bhatt, "Cavitation Damage at Elevated Temperature and Pressure," ASME 1972 Cavitation Forum, 11-13, 1972.

22. J. Z. Lichtman and D. H. Kallas, "Erosion Resistance of Coatings, Methods for Evaluating Erosion (Cavitation) Damage, Materials Protection, 6, 4, 40-45, April 1967.

23. G. M. Wood, L. K. Knudsen, and F. G. Hammitt, "Cavitation Damage Studies with Rotating Disk," Trans. ASME, 89, D, J. Basic Engr., 98-110, 1967.

24. R. Garcia and F. G. Hammitt, "Cavitation Damage and Correlations with Materials and Fluid Properties," Trans. ASME, 89, D, J. Basic Engr., 753-763, 1967.

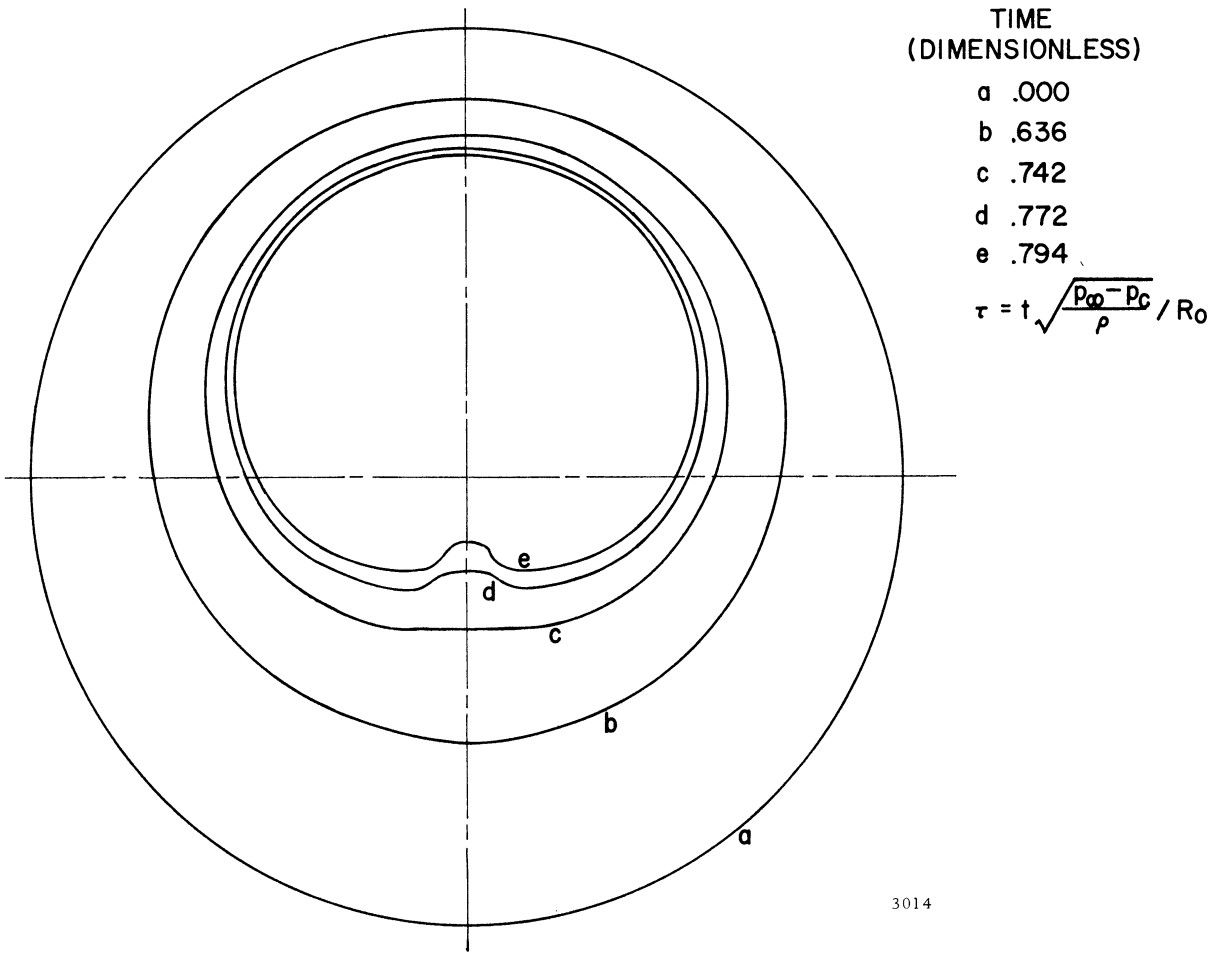

Fig. 1 **Bubble Wall Profile for Spherical Bubble Collapsing in Pressure Gradient, o = 0.19**

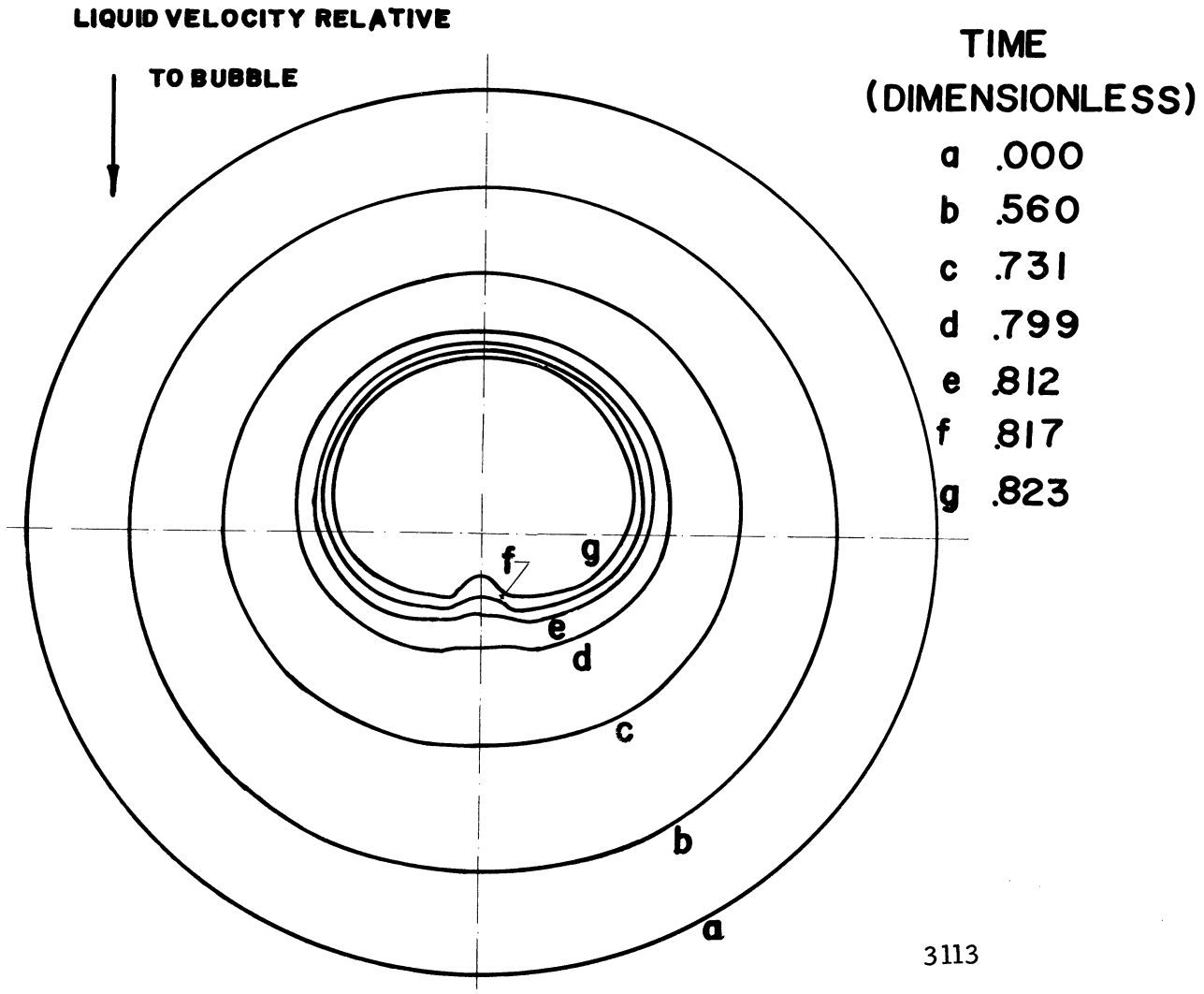

Fig. 2 Bubble Surface Profiles for Initially Spherical Bubble Moving Relative to Surrounding Liquid, $V_\infty = 0.1515$

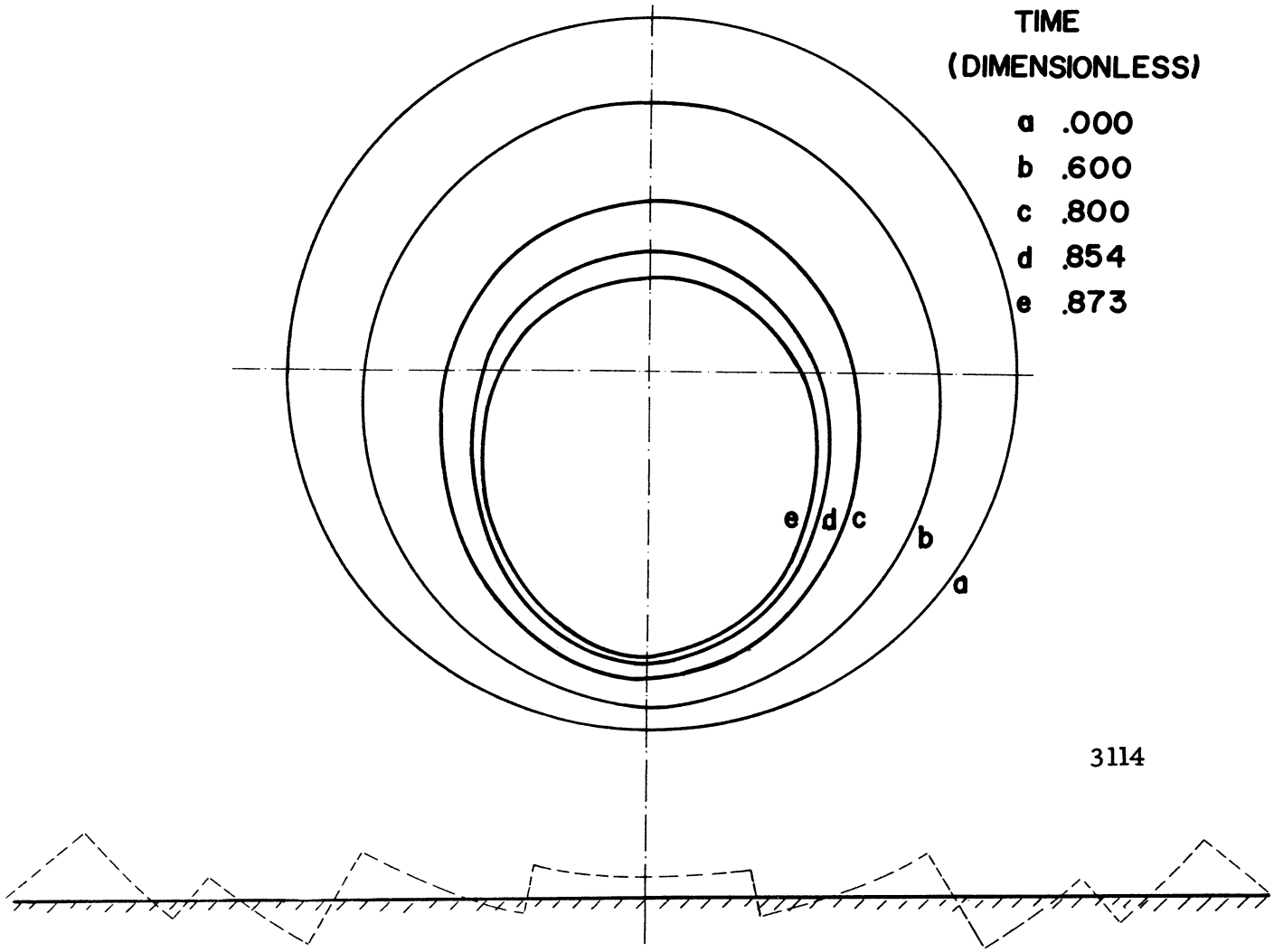

Figure 3 Bubble Surface Profiles for Initially Spherical Bubble with Center 1.5 R_o from Rigid Wall

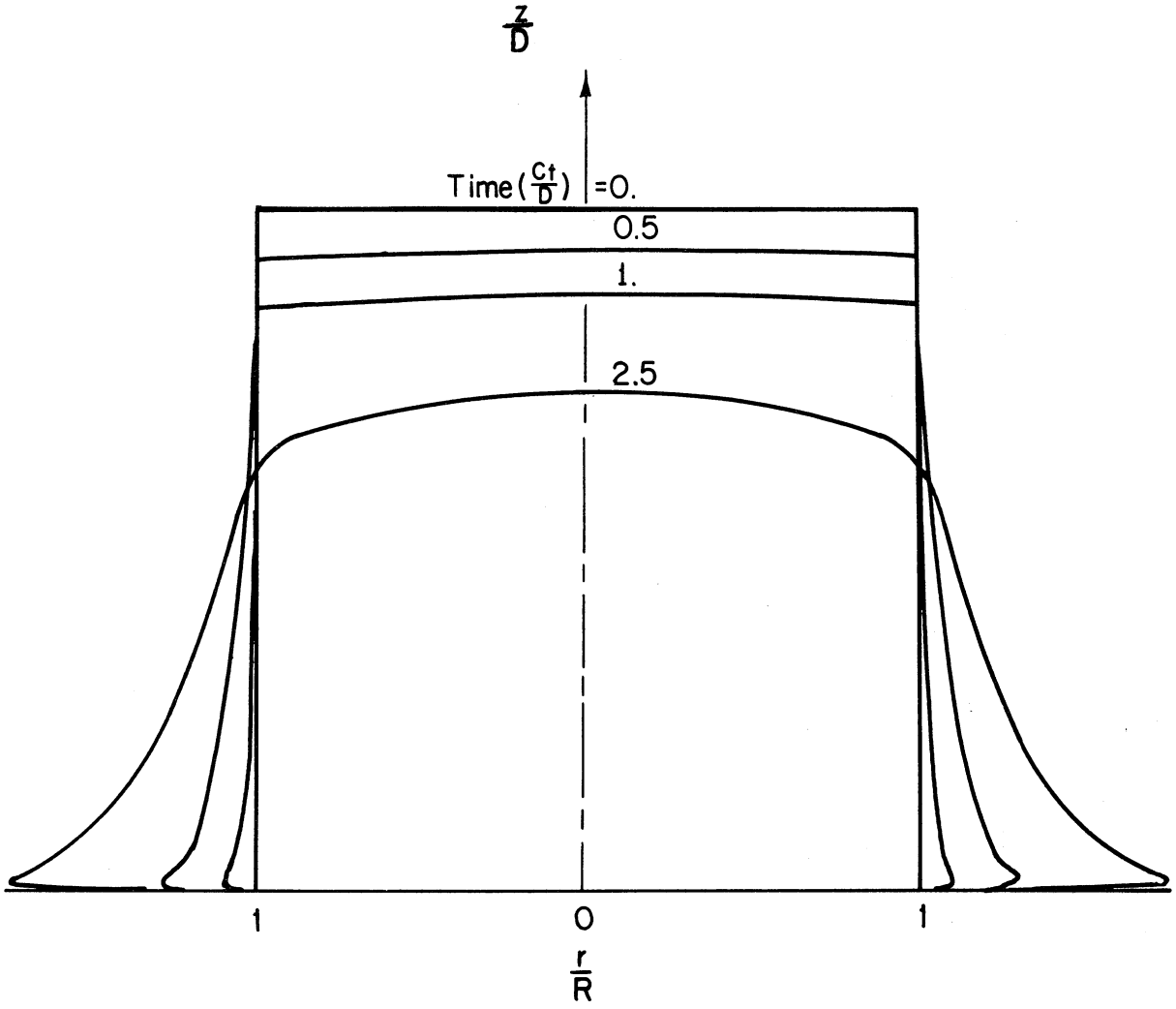

Fig. 4 Shape-Time History of an Initially Cylindrical Droplet with L/D = 1, at Mach Number = 0.2, for Free-Slip Boundary Condition.

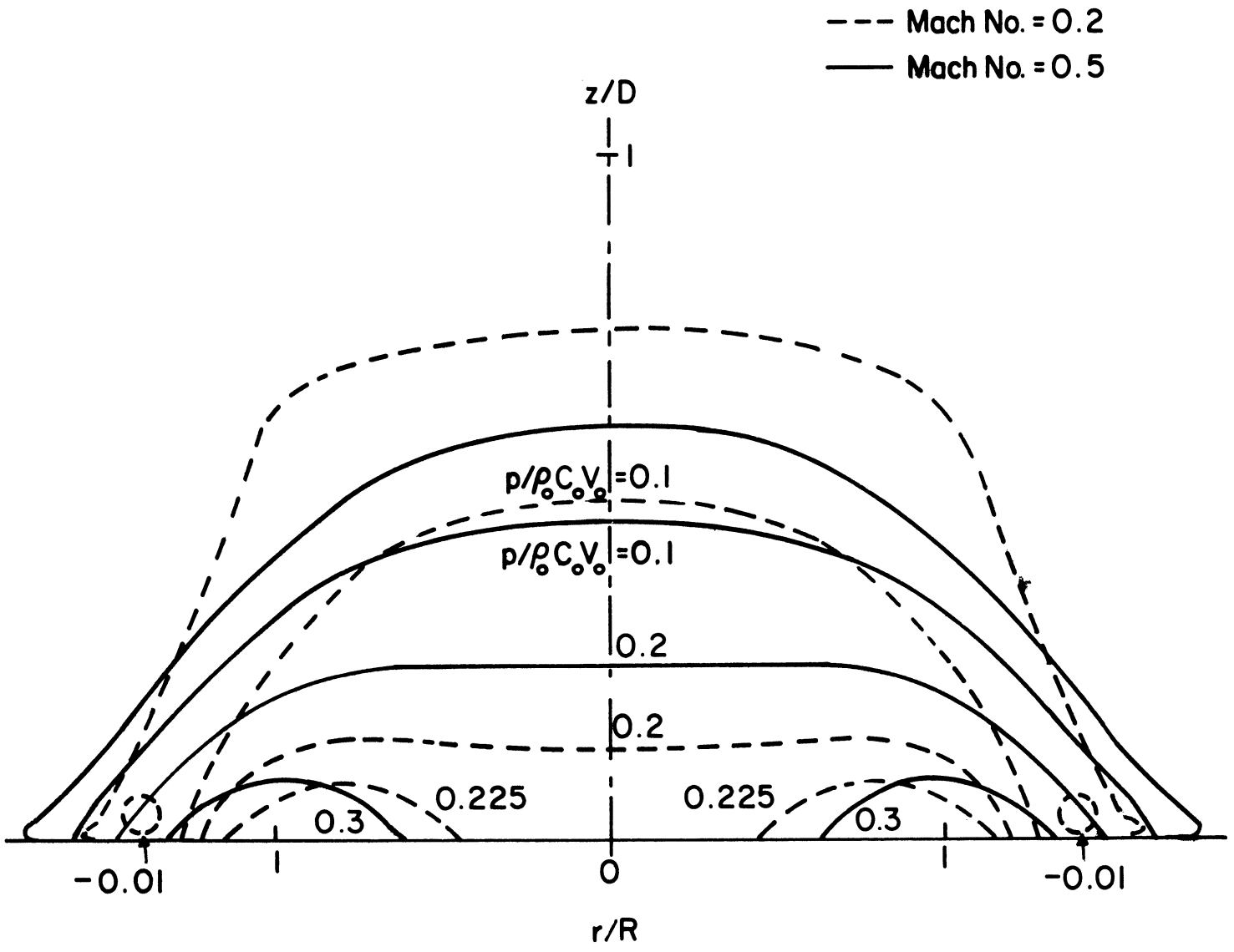

Fig. 5. Isobar Distribution in an Initially Cylindrical Droplet with L/D = 1, at Time (Ct/D) = 2.5, for Impact Mach Numbers of 0.2 and 0.5. Non-Slip Boundary Condition.

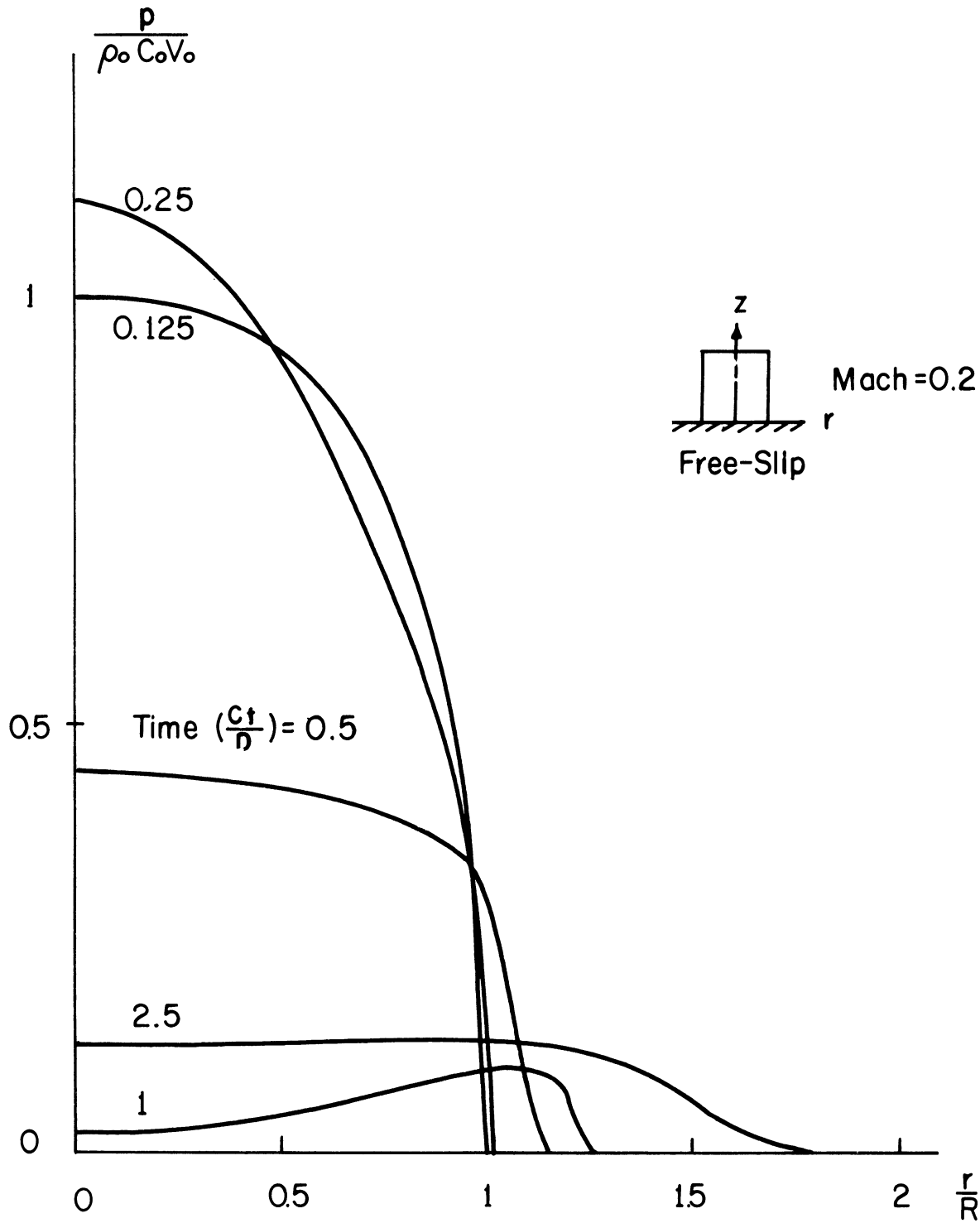

Fig. 6 Pressure-Time History at Liquid-Solid Interface (z = 0) of an Initially Cylindrical Droplet with L/D = 1, for Impact Mach Number of 0.2 and for Free-Slip Boundary Condition.

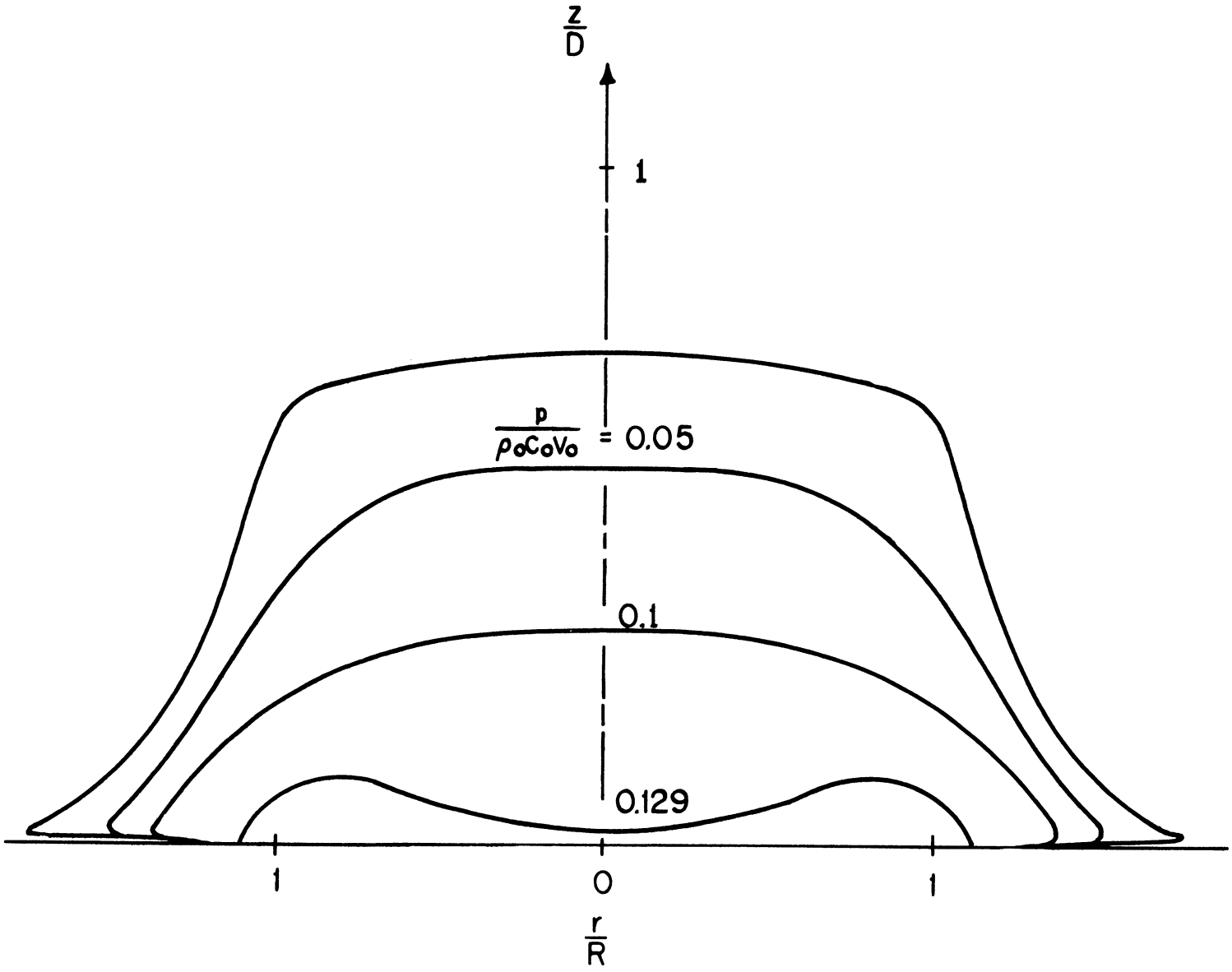

Fig. 7 Isobar Distribution in an Initially Cylindrical Droplet with L/D = 1, at Time (Ct/D) = 2.5, for Impact Mach Number of 0.2 and for Free-Slip Boundary Condition.

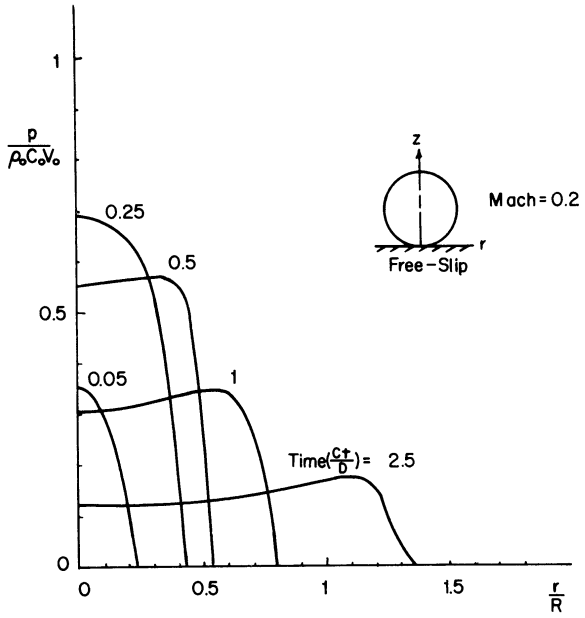

Fig. 8 Pressure-Time History at Liquid-Solid Interface (z=0) of an Initally Spherical Droplet for Impact Mach Number of 0.2 for Free-Slip Boundary Condition

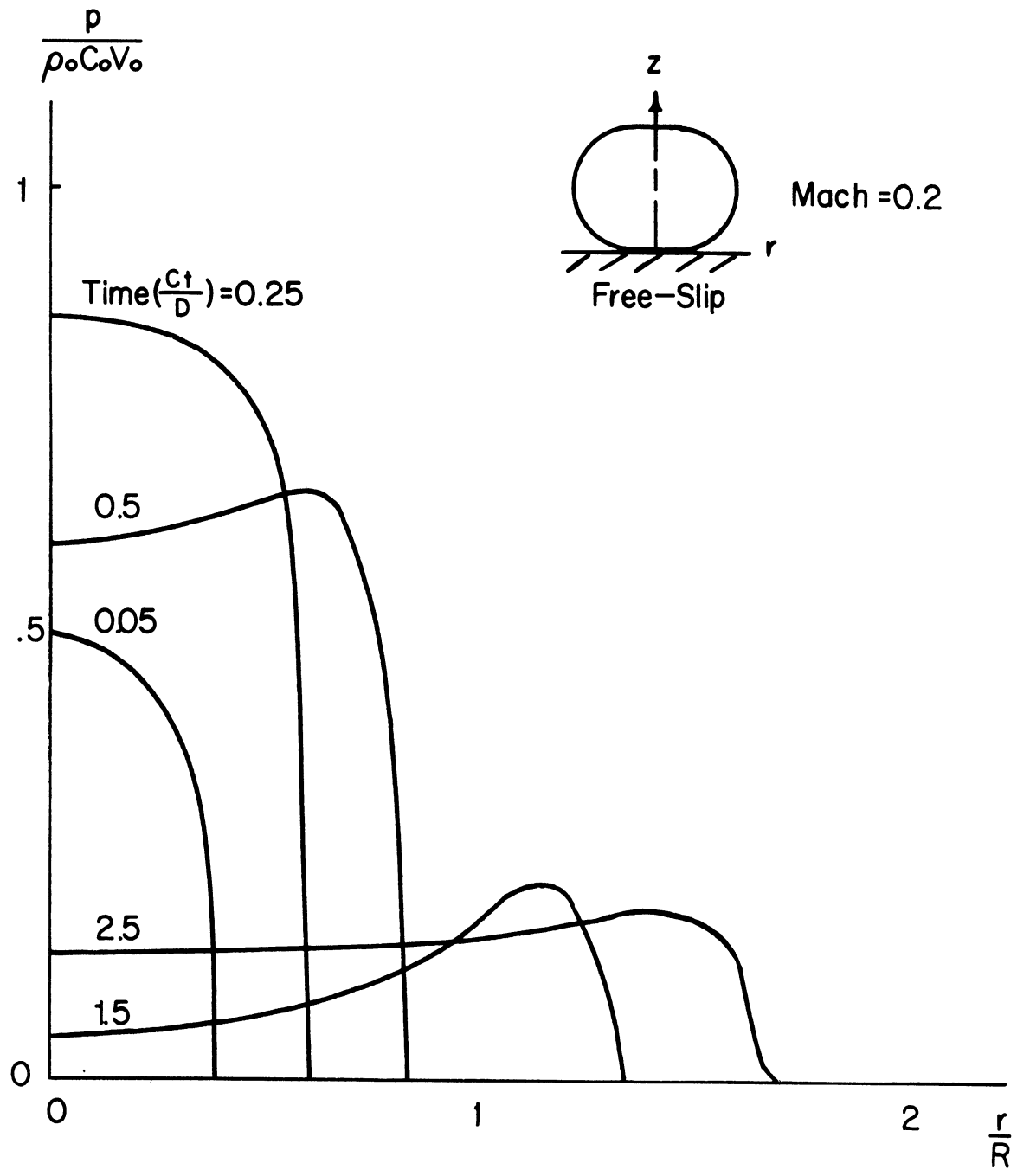

Fig. 9 Pressure-Time History at Liquid-Solid Interface (z=0) of an Initally Cylindrical-Spherical Composite Droplet with R/R=0.25 and L/D=1, for Impact Mach Number of 0.2 and for Free-Slip Boundary Condition

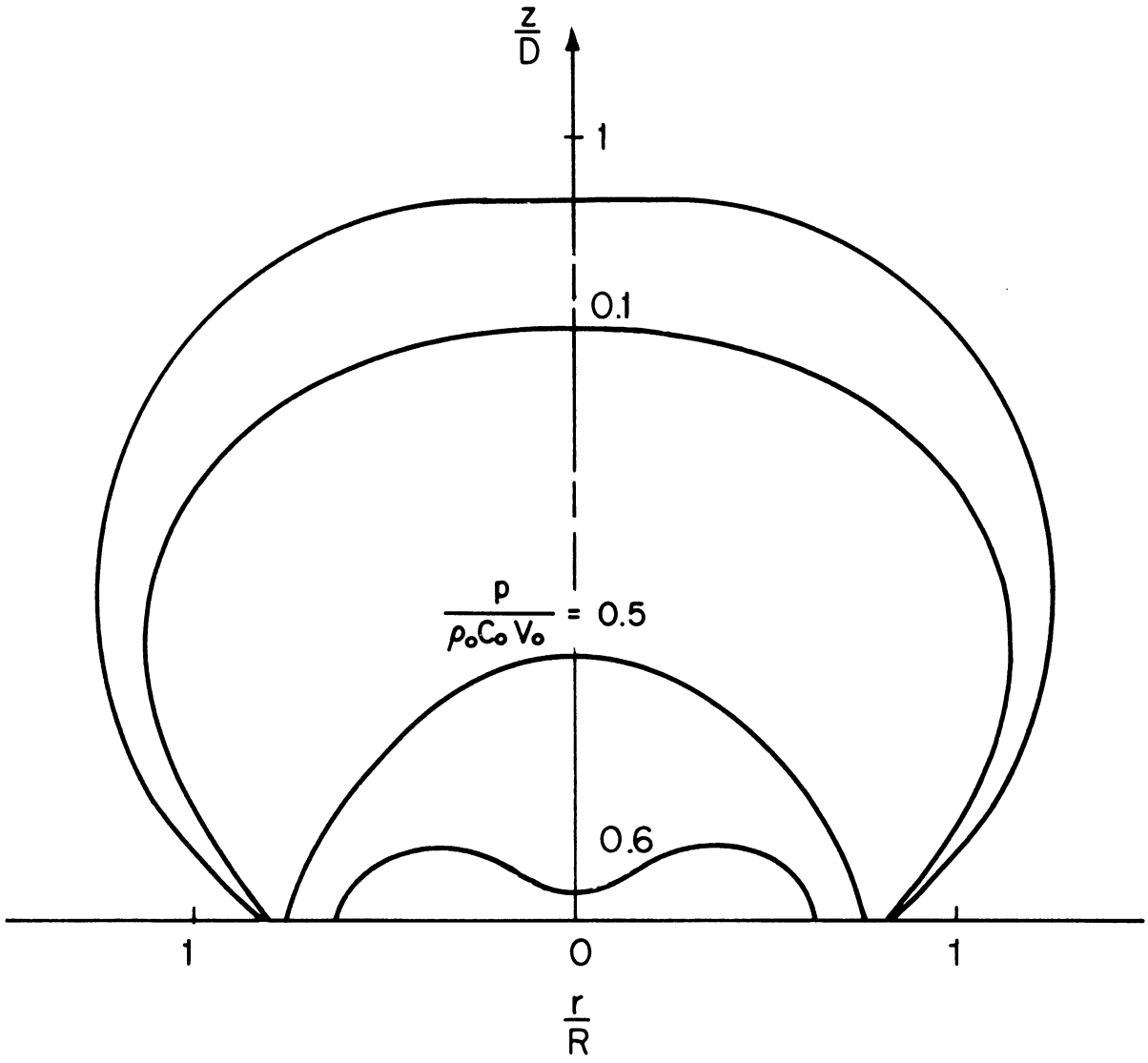

Fig. 10 Isobar Distribution in an Initially Cylindrical-Spherical Composite Droplet with $R_1/R = 0.25$ and $L/D = 1$, at Time $(Ct/D) = 0.5$, for Impact Mach Number of 0.2 and for Free-Slip Boundary Condition.

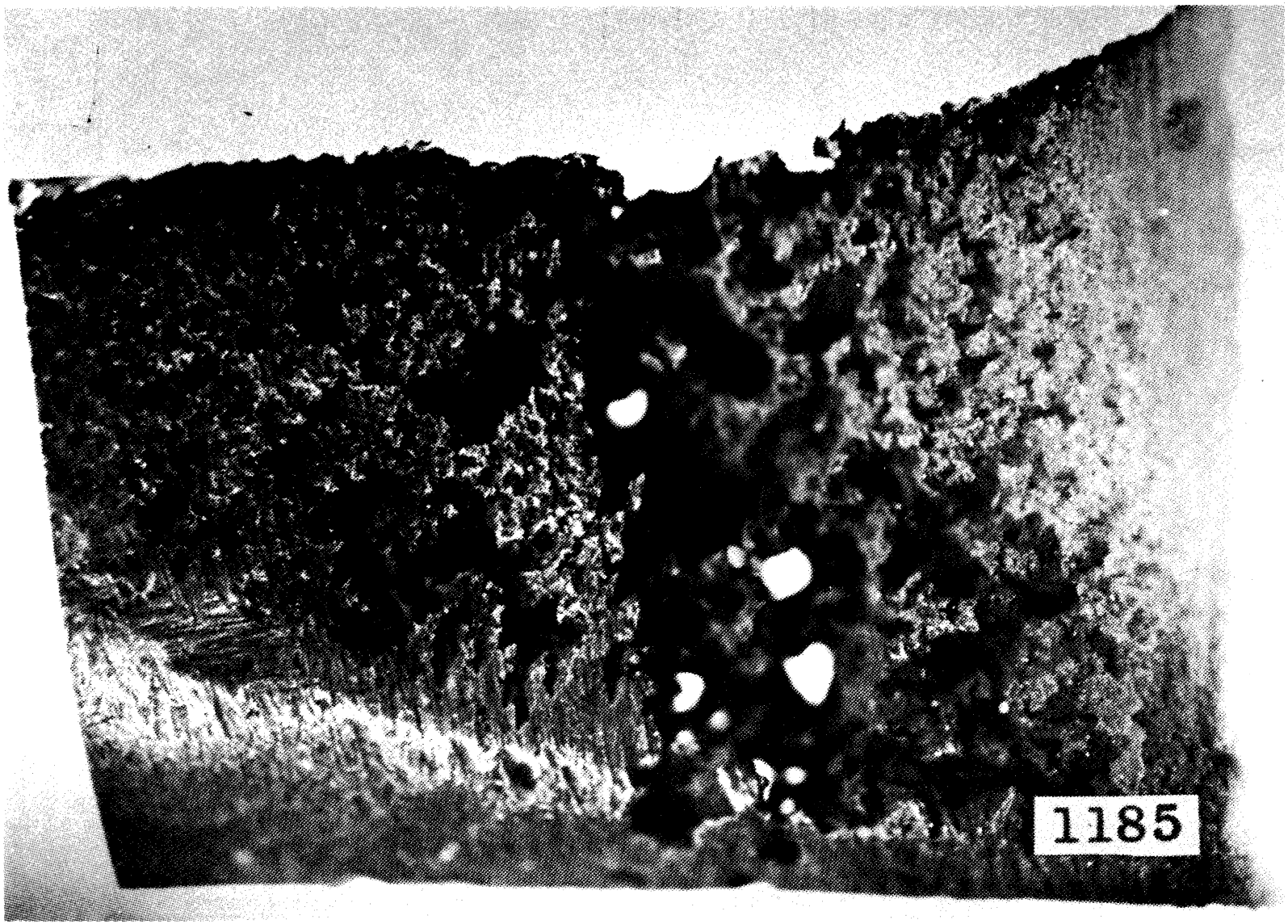

Fig. 11 **Cavitation Erosion - Boiler Feed Pump**

1174

Fig. 12 **Cavitation Erosion - Mercury Pump**

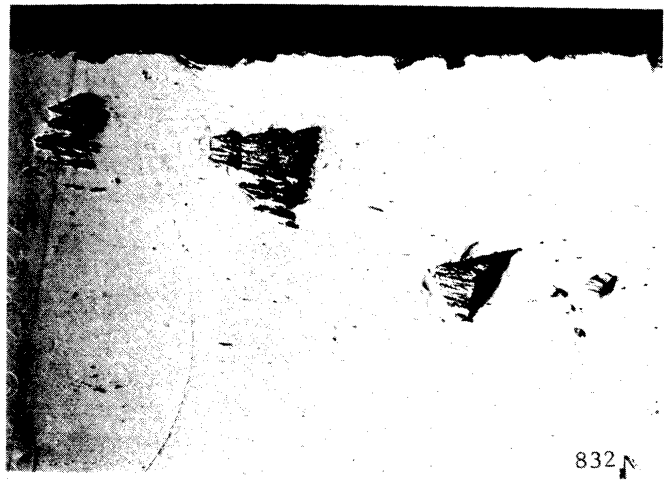

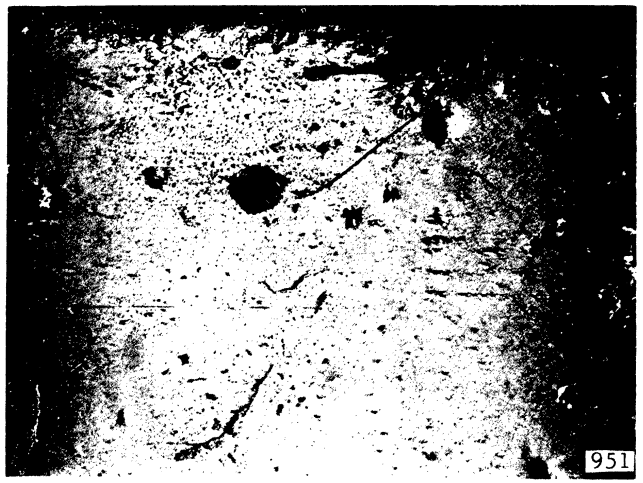

(a) (b)

FIG. 13-a. Development of Cavitation Damage at Two Locations on 302 Stainless Steel Specimen with Water: (a) Early in test; (b) later in test (150 hrs).

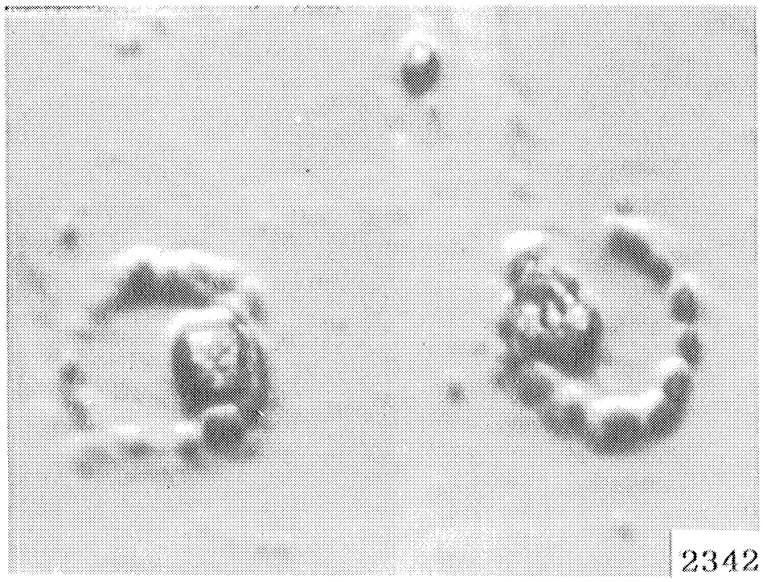

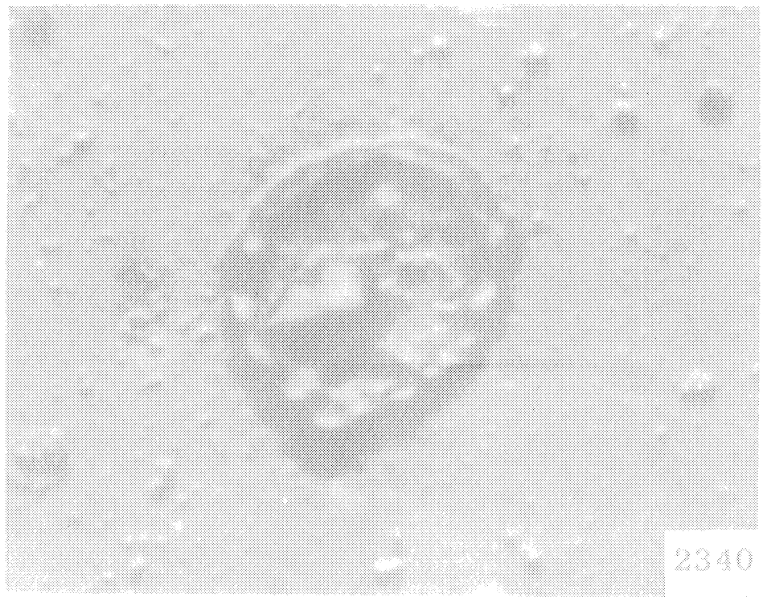

FIG. 13-b. Single Blow Cavitation Craters, Plexiglas

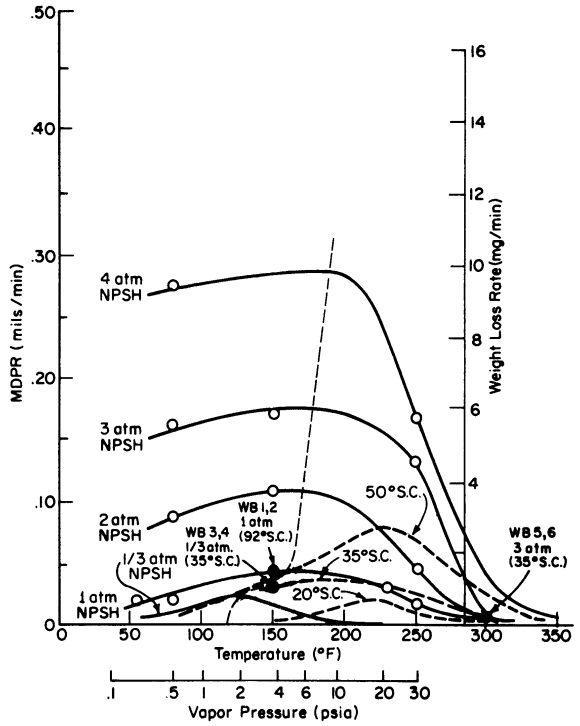

Fig. 14 Pressure Effect in Vibratory Tests. Maximum Volume Loss Rate for Bearing Brass SAE-660 vs. Temperature and Vapor Pressure

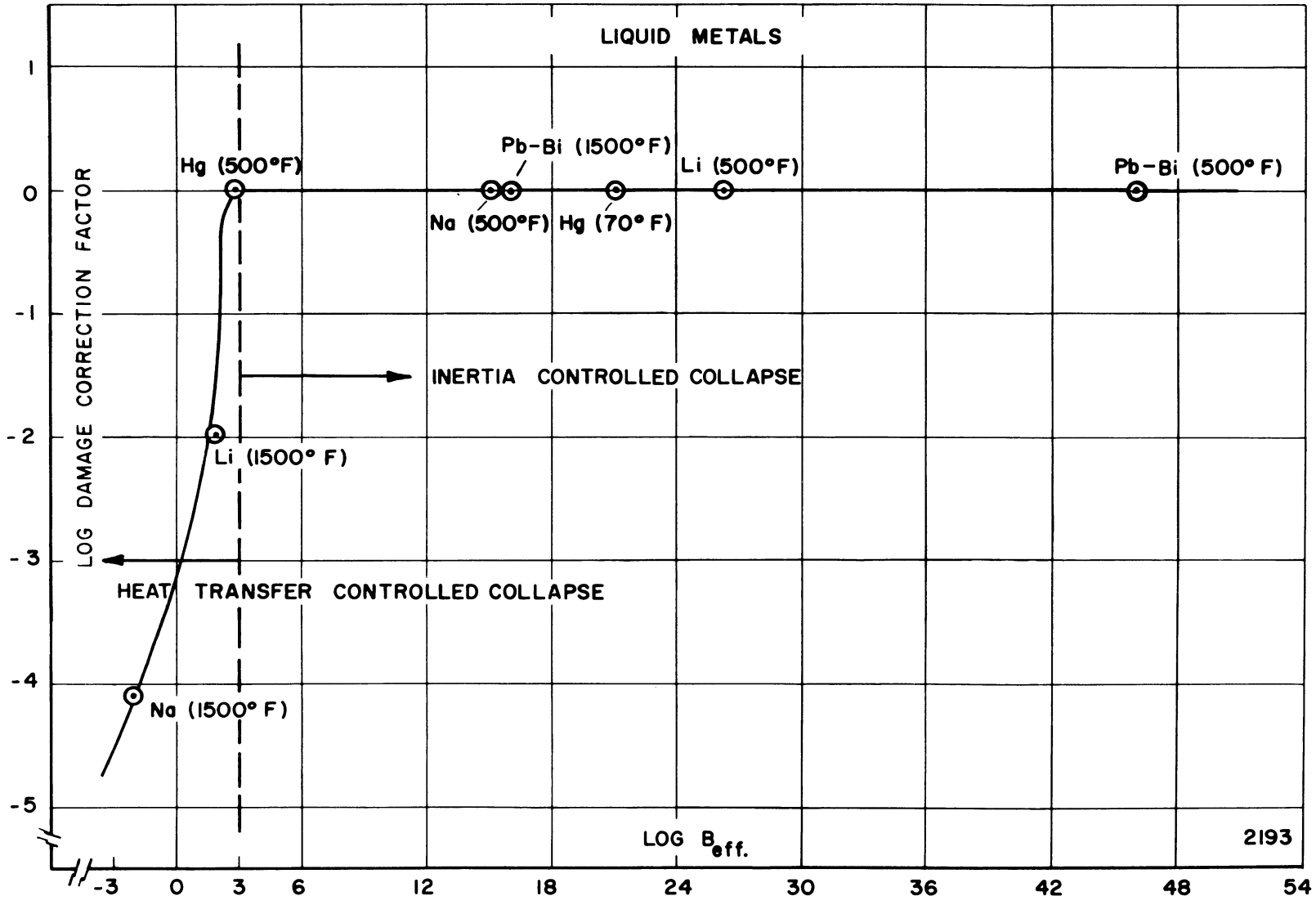

Fig. 15. Liquid Metal Temperature Effect in Vibratory Test

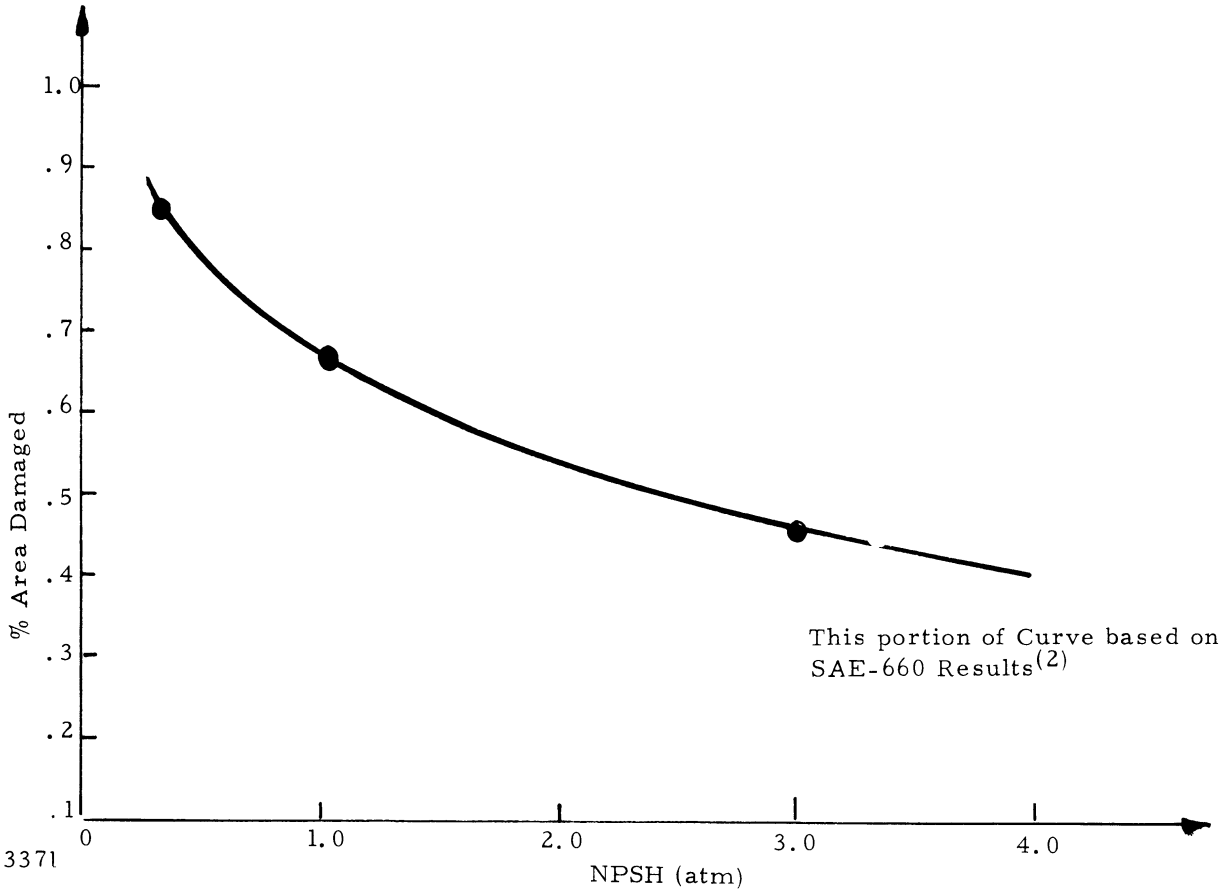

FIG. 16-a. Effect of Pressure on Damage Pattern: Area Damaged vs. NPSH

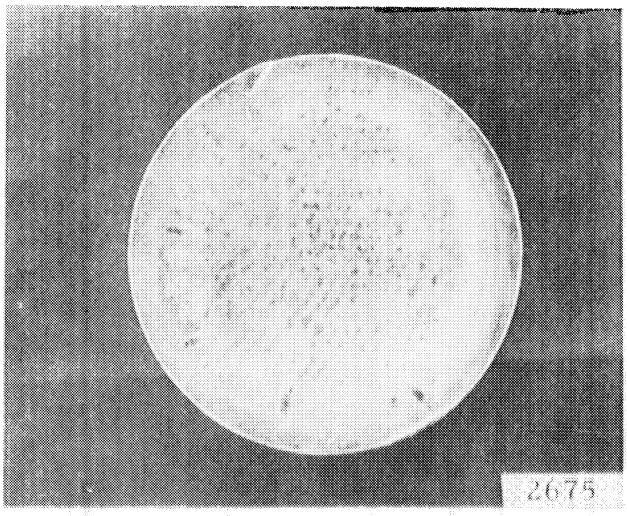

Specimen No. : II-1-M
Pressure: 1 atm. NPSH
Duration: 60 min.
Weight Loss: 59.5 mg.

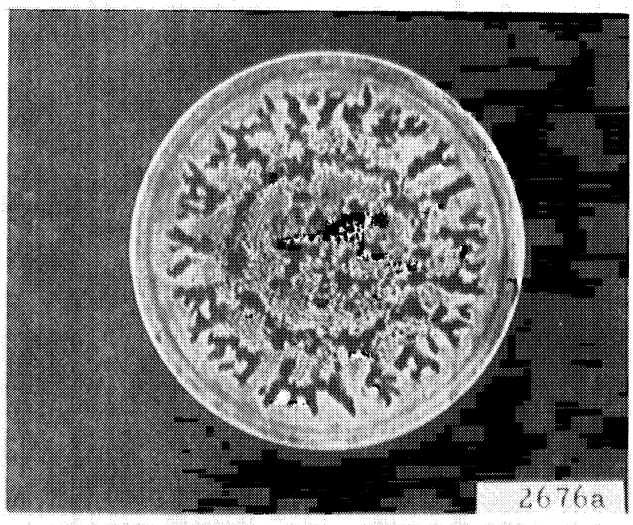

Specimen No. : N-5
Pressure: 2 atm. NPSH
Duration: 90 min.
Weight Loss: 144 mg.

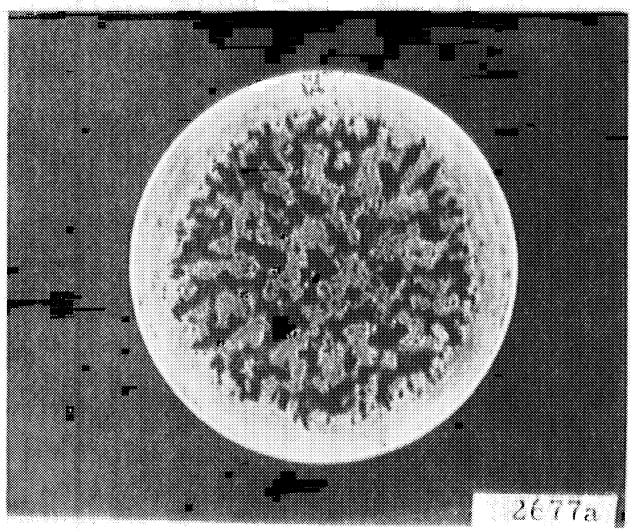

Specimen No. N-7
Pressure: 3 atm. NPSH
Duration: 90 min.
Weight Loss: 219 mg.

FIG. 16-b. Effect of Pressure on Damage Pattern: Photos of Damaged Specimens Tested at Different Pressures

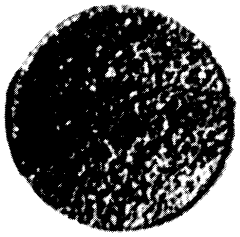

(1) 12 Hour Exposure
Pb-Bi at 500°F

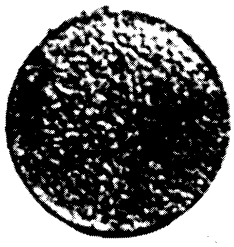

(2) 6 Hour Exposure
Pb-Bi at 1500°F

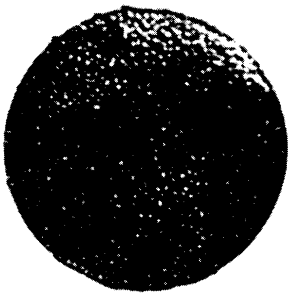

(3) 12 Hour Exposure
Mercury at 500°F

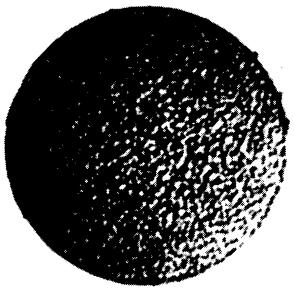

(4) 12 Hour Exposure
Mercury at 70°F

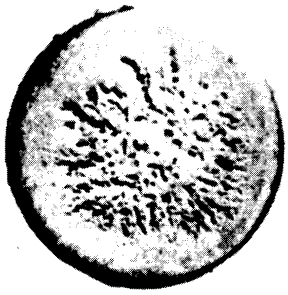

(5) 36 Hour Exposure
Water at 70°F

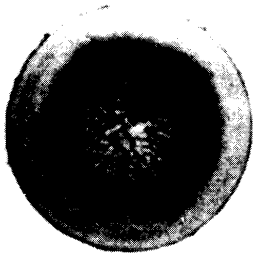

(6) 10 Hour Exposure
Lithium at 500°F

2818

FIG. 16-c. Effect of Pressure on Damage Pattern: Photos of Damaged Specimens Tested in Fluids of Differing Density

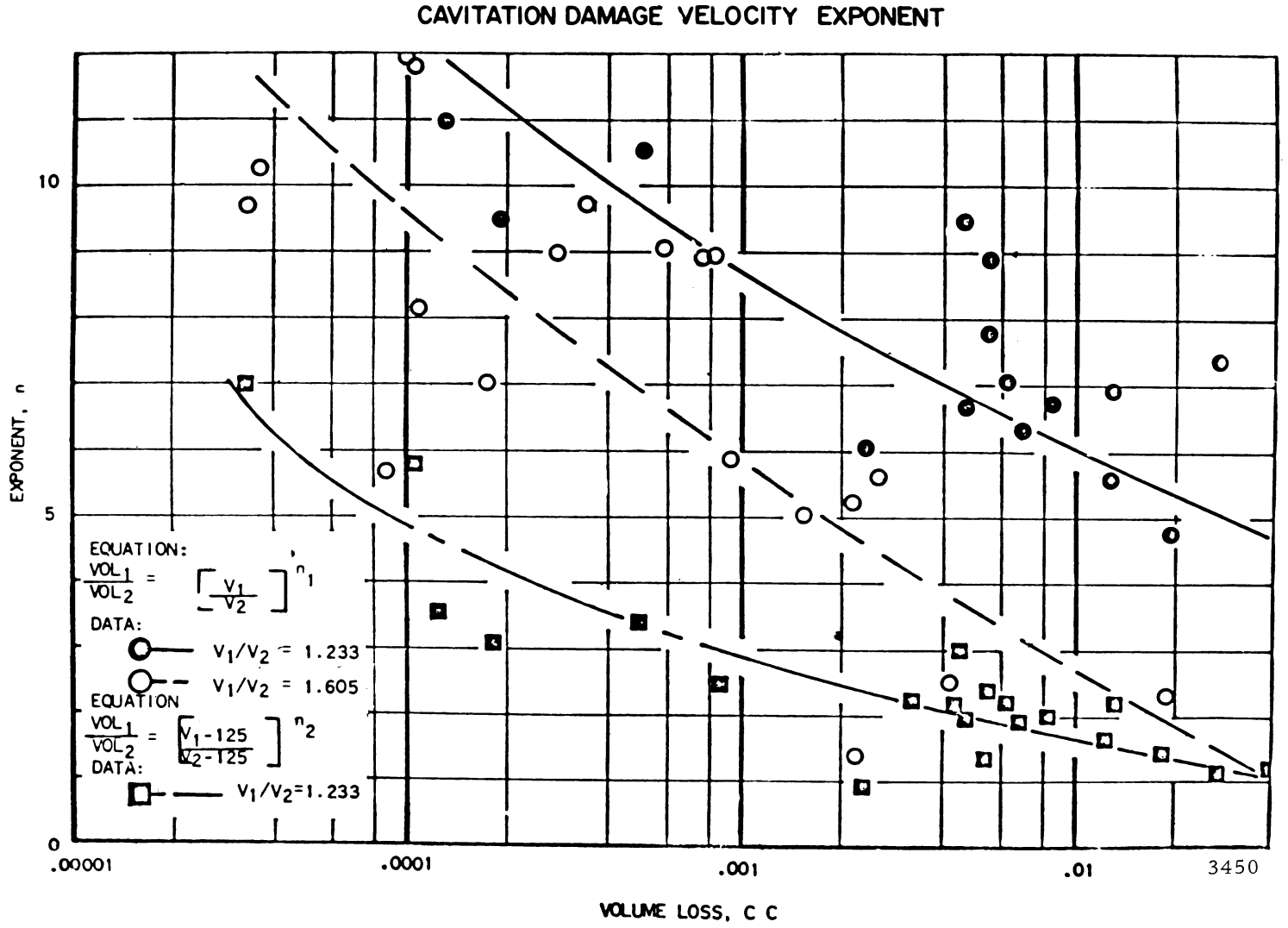

Fig. 17 Velocity Effect on Cavitation Damage, Rotating Disc Tests, Pratt and Whitney Aircraft (23)